Towards high-fidelity simulations for external aerodynamics of industry relevant cases

Ivette Rodríguez

ivette.rodriguez@upc.edu

With the collaboration of: O. Lehmkuhl, B. Eiximeno, R. Montalà, J.M. Duró, R. Borrell, A. Lozano-Durán, R. Vinuesa, B. Font, A. Miró

UNIVERSITAT POLITÈCNICA DE CATALUNYA BARCELONATECH

TUAREG Turbulence and Aerodynamics Research Group

TUAREG (UPC) Group

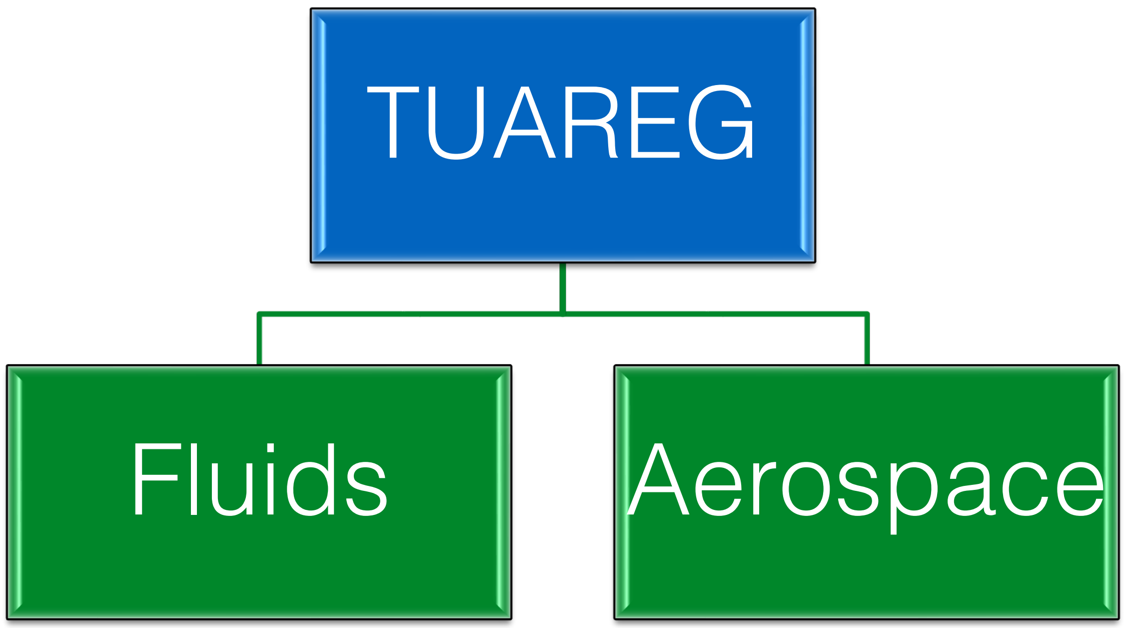

- 15 full-time professors
- 2 Research Engineers
- 10 PhD students

Tuareg Fluids division

Use and improvement of existing industrial numerical simulation tools, deepening on the knowledge of fluid dynamics, turbulence modelling, and heat transfer.

High Performance Computing in basic and applied research on Mechanical and Aeronautical Engineering fields

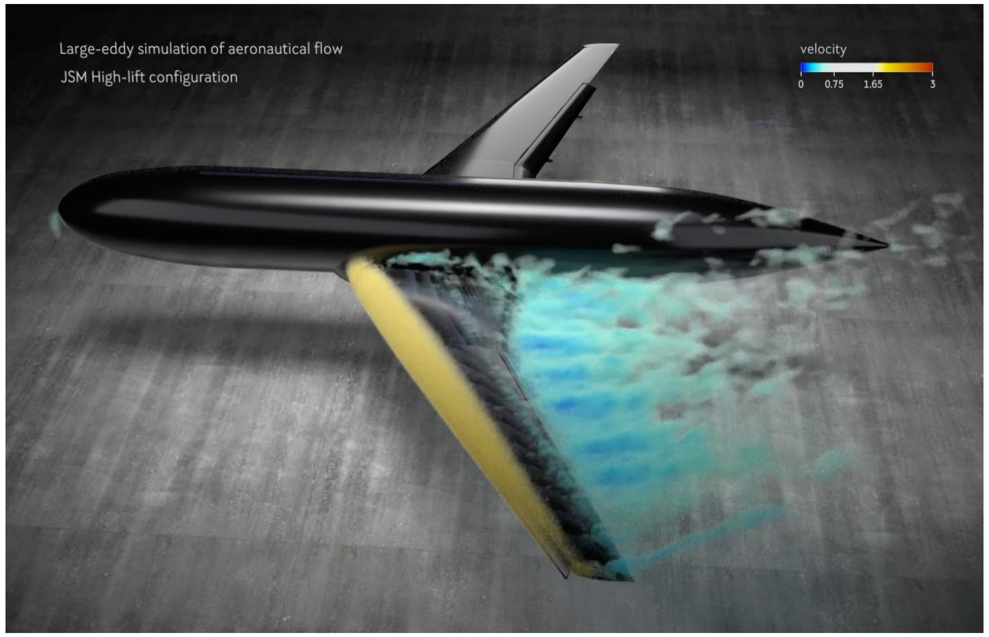

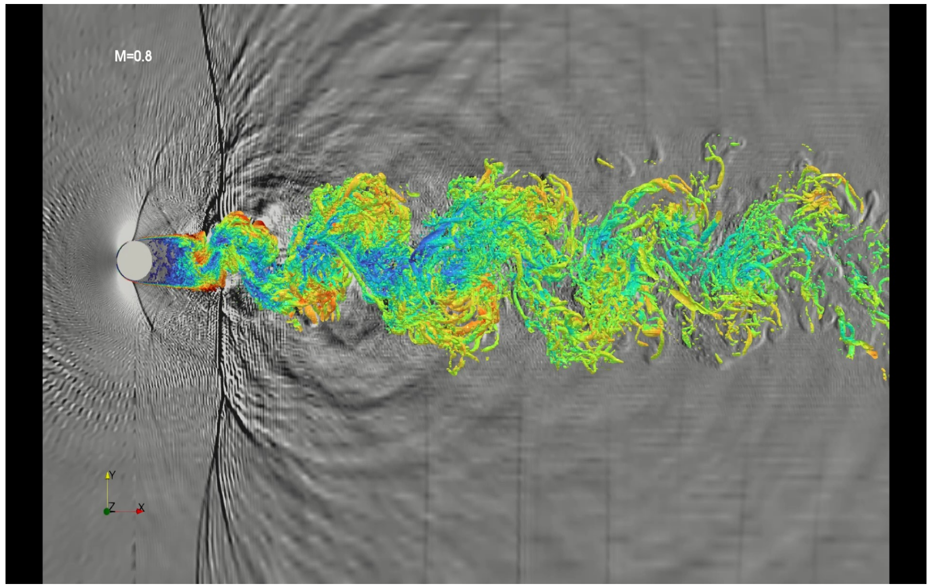

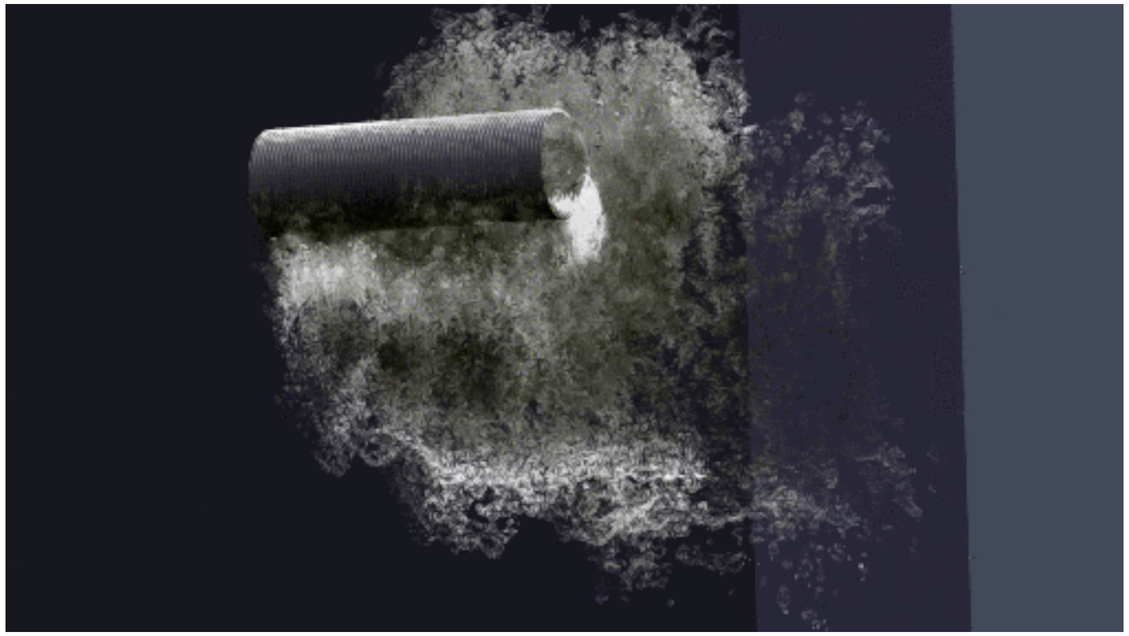

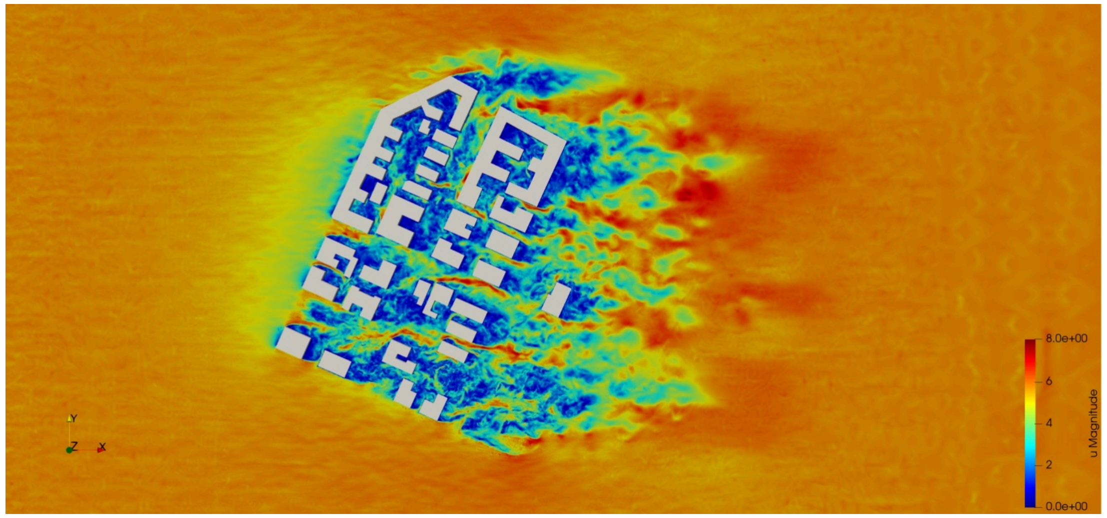

Introduction / Motivation

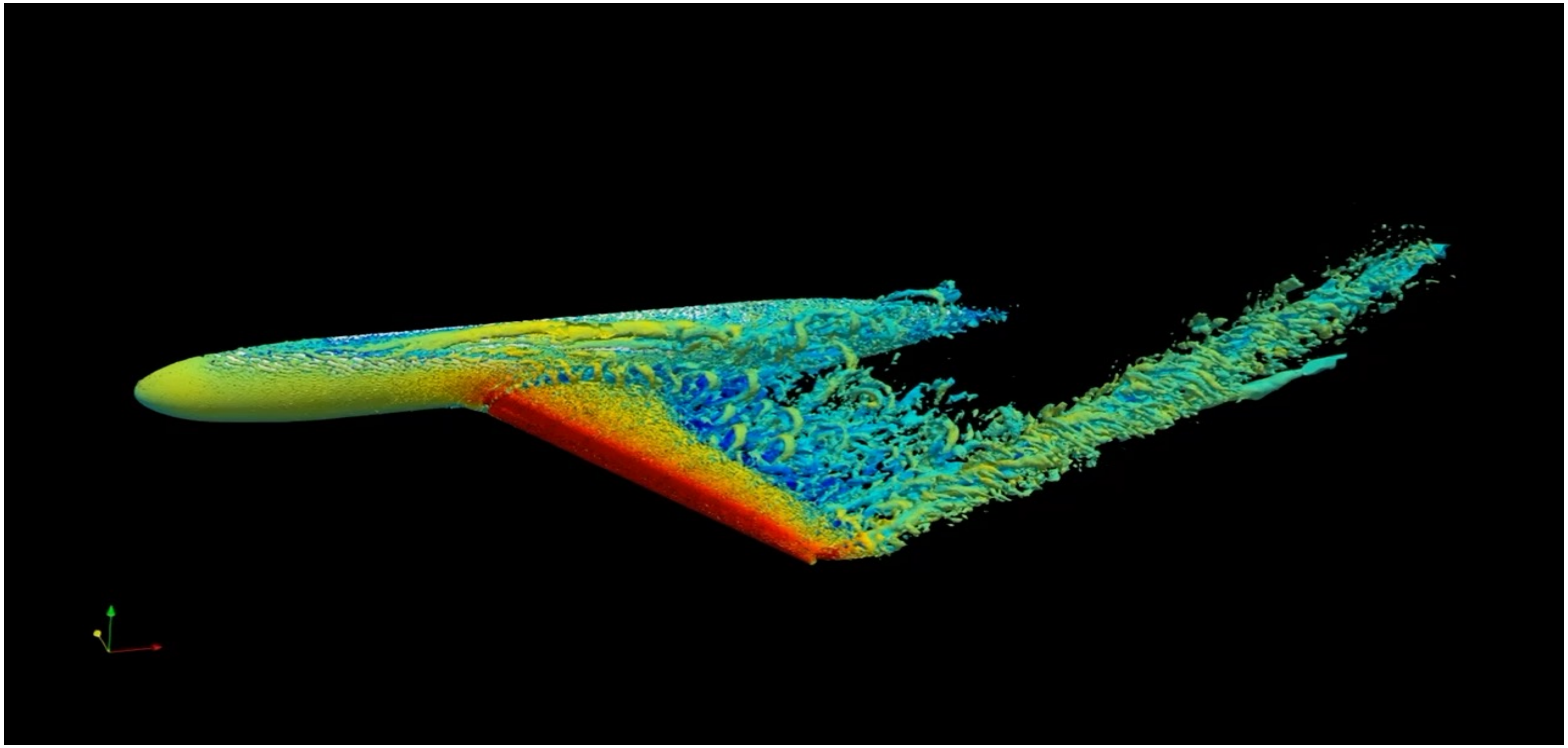

- ❑ Turbulence is a very complex phenomena, present in industrial applications e.g., the aerodynamic efficiency of an aircraft is affected by the interaction with the nacelle, brackets, fairings, … specially at high AoA (take-off & landing)
- ❑ Turbulent structures, specially those in the BL, are responsible for the viscous drag and aerodynamic noise

Video data from: Lehmkuhl, O., Lozano-Durán, A. and **Rodríguez, I.** (2020).

Introduction / Motivation

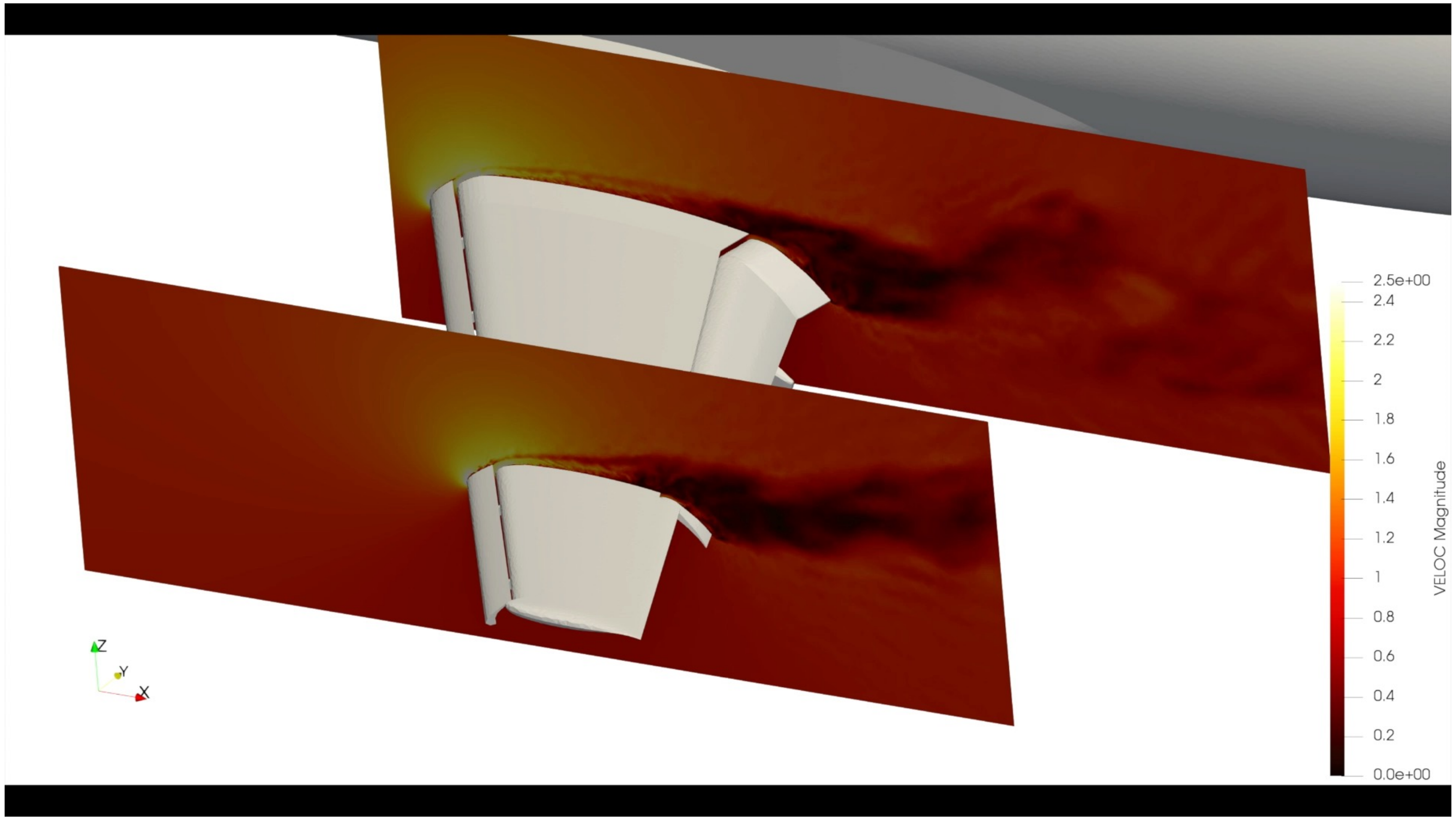

- ❑ **Can we accurately solve turbulence interactions in complex geometries at industry relevant Reynolds numbers?**
- ❑ **How to tackle this phenomenon**
- ❑ **Which are the challenges?**
- ❑ **Data analysis and the new technologies**

Video data from: Lehmkuhl, O., Lozano-Durán, A. and **Rodríguez, I.** (2020).

Outline

- ❑ Technical challenges for scale resolving applications
- ❑ Numerical approach - Low-dissipation schemes
- ❑ Applications: WRLES, flow control
- ❑ Data analysis: Reduced order models

Technical approach - challenges

- To solve all the flow scales (**DNS**) of real word problems is not feasible with the current HPC machines (including exascale machines)
- Two main strategies have been adopted by the community:
  - **RANS**: to time average the flow and solve an equivalent steady state problem (**industrial standard/low HPC needs**).
  - **LES**: to partially solve the spatial scales and fully solve the transient dynamics (**basic research standard/high HPC needs**).

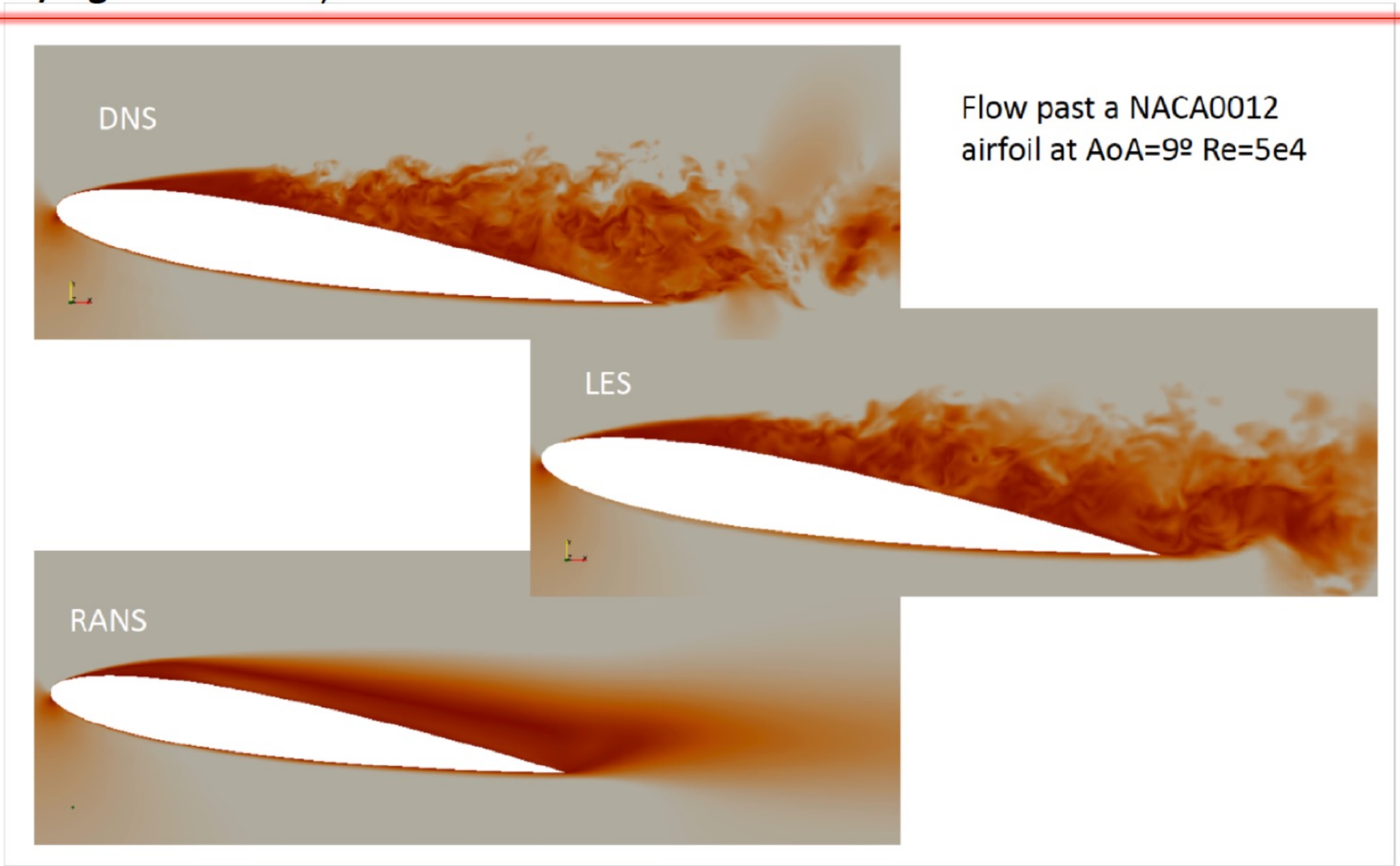

I. Rodriguez et al. C&F 2013

Technical approach - challenges

Numerics & modelling

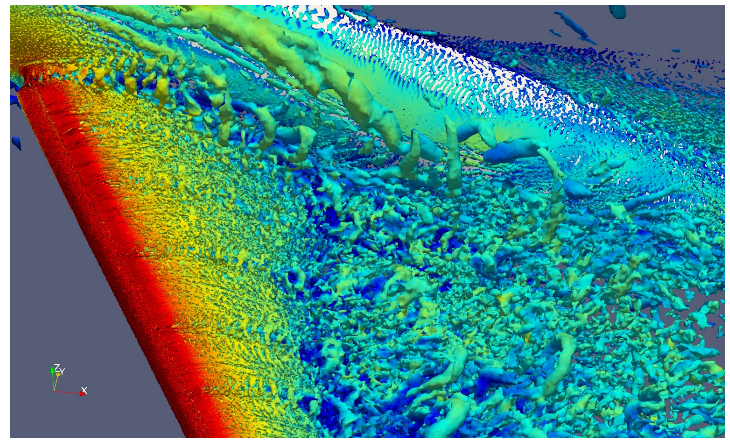

Wall-resolved LES
Re=7.5x10^5

Wall-modelled LES
Re=4.87x10^6

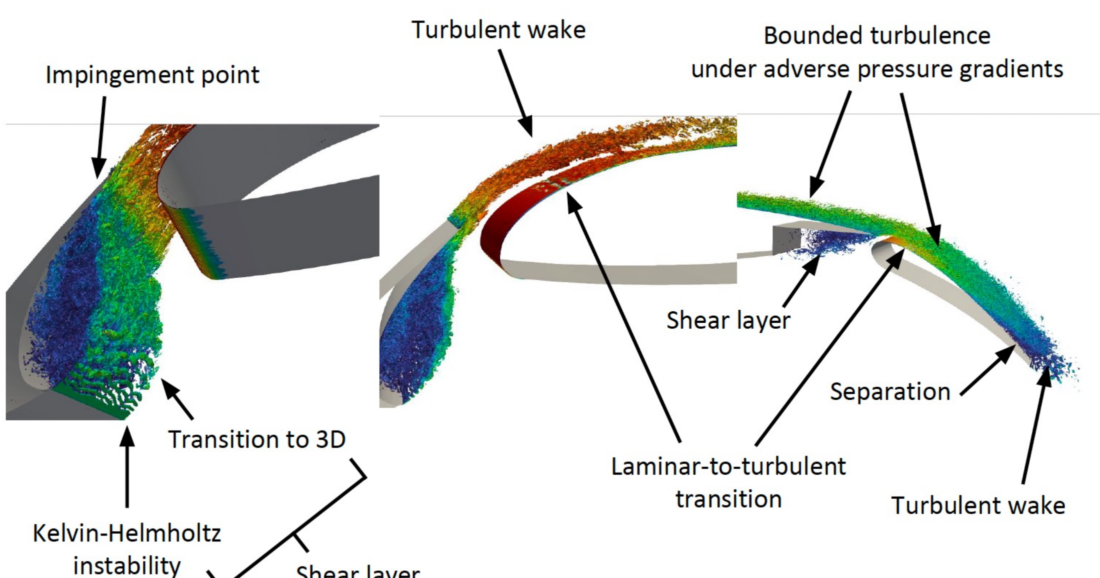

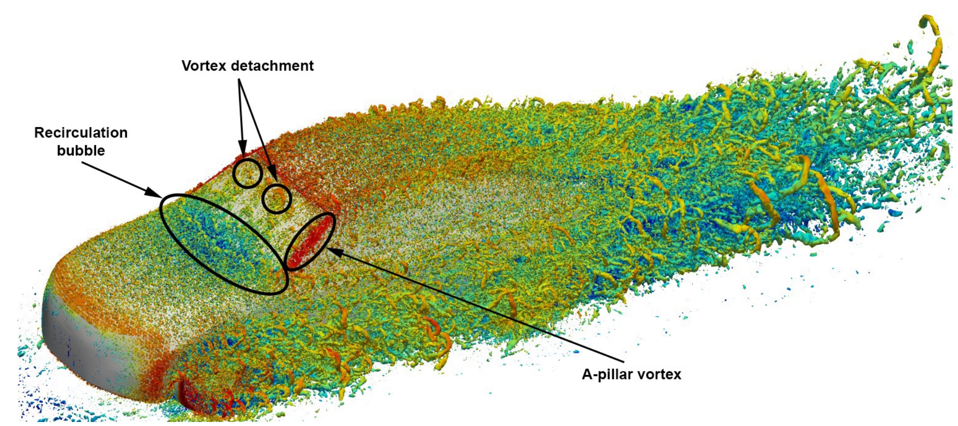

***Q criterion iso-surfaces at α = 9º**. Results presented at Montalà, R.; Eiximeno, B.; Miro, A.; Lehmkuhl, O.; Rodriguez, I. Turbulent Boundary Layer in a 3-Element High-Lift Wing: Coherent Structures Identification. *DLES13 Direct and Large Eddy Simulations*, Udine, Italy, 2022

- Technical challenges for scale resolving applications
- **Numerical approach - Low-dissipation schemes**
- Applications: WRLES, flow control
- Data analysis: Reduced order models

Numerical approach

$$\frac{\partial \overline{u}_i}{\partial x_i} = 0$$

$$\frac{\partial \overline{u}_i}{\partial t} + \frac{\partial \overline{u}_i \overline{u}_j}{\partial x_j} - \nu \frac{\partial^2 \overline{u}_i}{\partial x_j \partial x_j} + \rho^{-1} \frac{\partial \overline{p}}{\partial x_i} - F_i = -\frac{\partial \mathcal{T}_{ij}}{\partial x_j}$$

$$\mathcal{T}_{ij} - \frac{1}{3}\mathcal{T}_{kk}\delta_{ij} = -2\nu_{sgs}\overline{S}_{ij}$$

Specific challenges:

- ❑ **Unstructured grids, usually the mesh is the filter**
- ❑ **Numerics interact with the LES model**
- ❑ Scales at the wall are case dependent
- ❑ More sensible to geometry and boundaries

- Smagorinsky ✗
- Dynamic Smagorinsky ✗
- Wall-Adapting Local Eddy-Viscosity (WALE) Model ✓
- **Vreman:** ✓
- **ILSA** ✓

Numerical approach: LES + low dissipation

Alya

Low dissipation FEM

Convective term	Energy	Momentum	Angular momentum
Non-conservativ e	-	-	-
Skew-symmetric	X	-	-
EMAC	X	X	X

Lehmkuhl, O., Houzeaux, G., Owen, H., Chrysokentis, G., Rodriguez, I., 2019. JCP 390, 51-65.

SOD2D

- Spectral formulation of Continuous Galerkin FEM applied to the spatial terms in the Navier-Stokes equations
- The Lobatto-Gauss-Legendre (LGL) quadrature is used (nodes are non-equispaced), avoiding the Runge effect on high-order interpretation
- Entropy viscosity model* is used for stabilization
- Time integration: explicit 4th order RK

https://gitlab.com/bsc_sod2d/sod2d_gitlab

L. Gasparino, F. Spiga, and O. Lehmkuhl, \Sod2d:," Computer Physics Communications, vol. 297, p. 109067, 2024.

Numerical approach: WMLES validation

D within the inner portion of the boundary layer

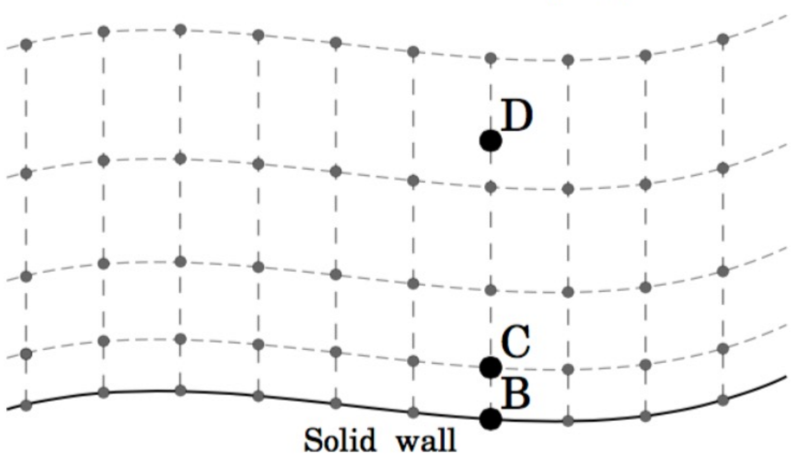

B-C Standard FD

B-D Exchange location (Kawai & Larsson)

NACA 4412, Re 1M, AoA = 5º

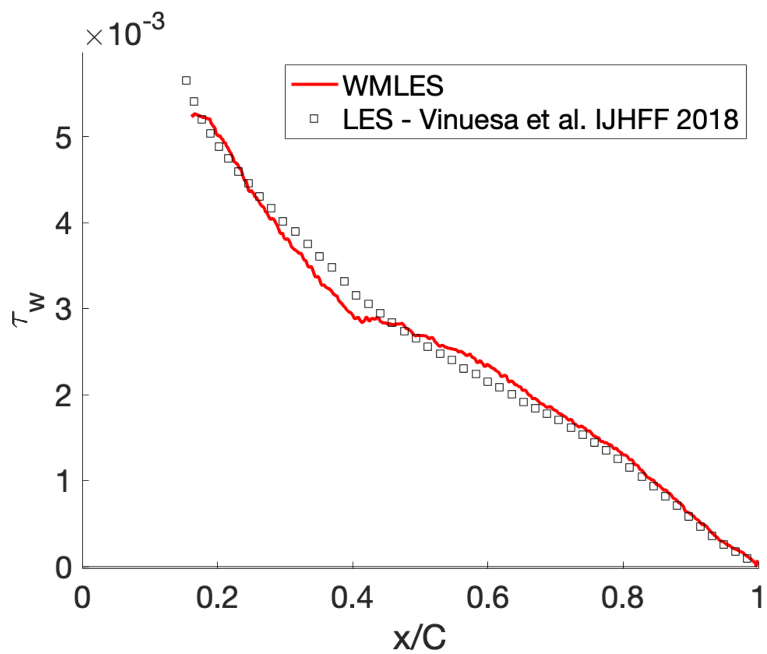

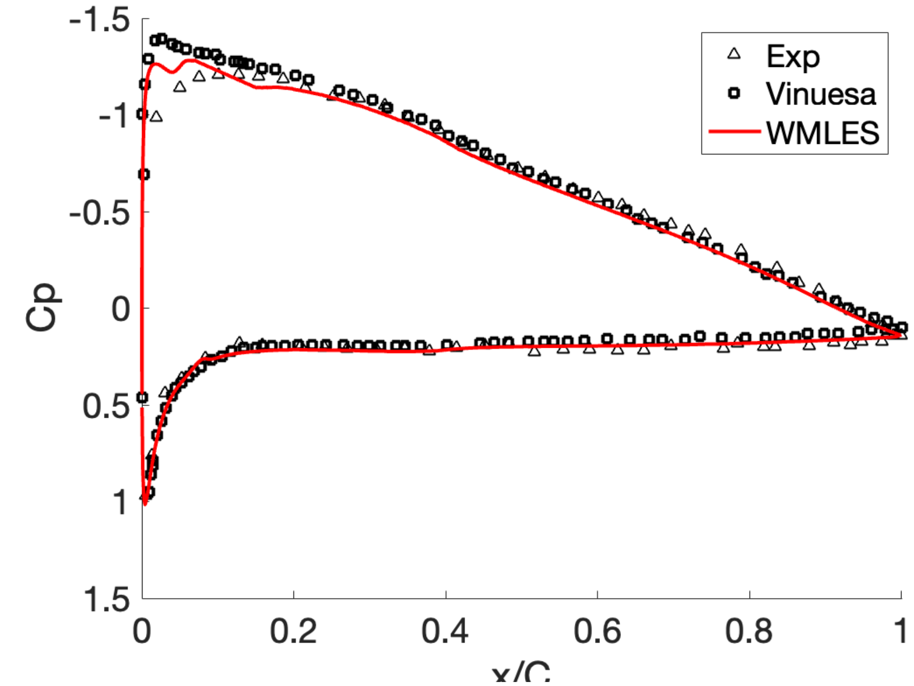

Set the velocity to zero at the wall
and
modify the viscosity in the first element such that

$$\tau = \mu_{first-element} \frac{\partial u_t}{\partial n}$$

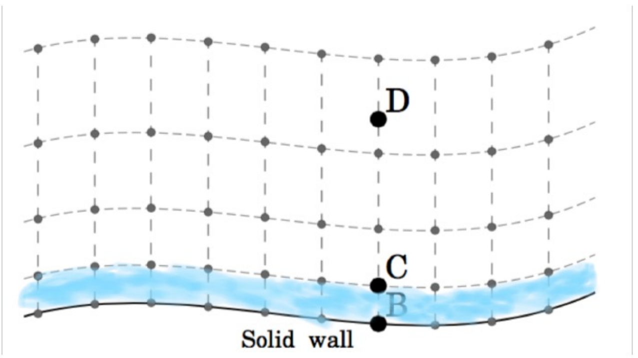

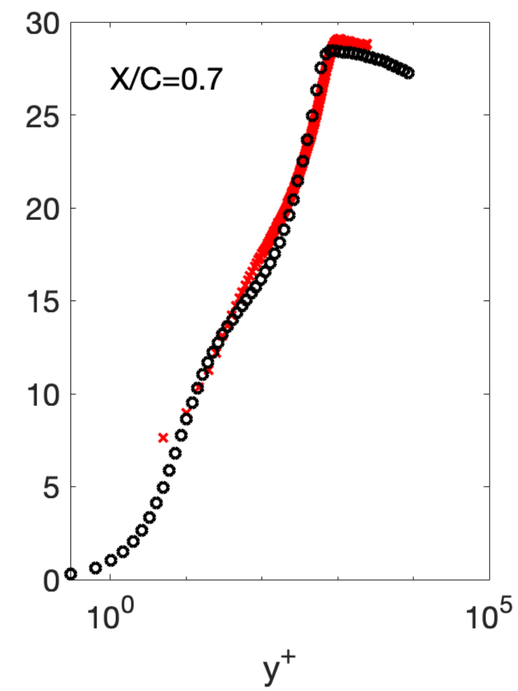

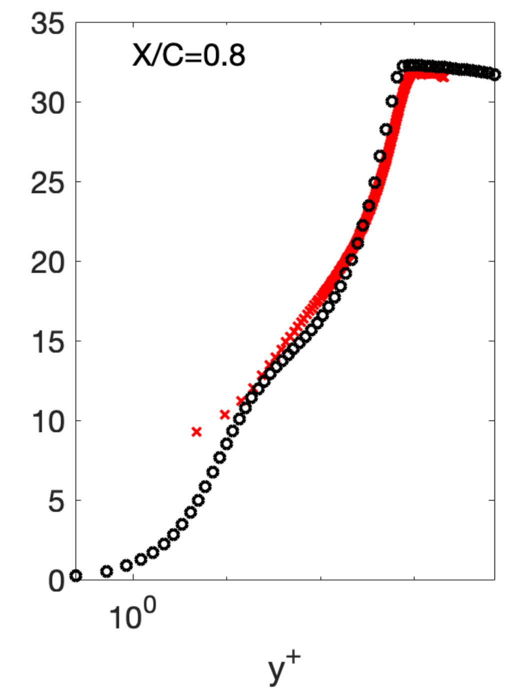

- Traction from wall law input — input instantaneous or average velocity at exchange location (C or D)
- Tangential velocity gradient in the normal direction
- We thus obtain the viscosity to be used in the first element.

LES data - R. Vinuesa et al.. Turbulent boundary layers around wing sections up to Rec = 1000000. Int. J. Heat Fluid Flow, 72:86–99, 2018.
Exp data - [1] J. Wadcock, "Investigation of low-speed turbulent separated flow around airfoils," 1987.

Validation: WMLES

- DrivAer model
- Fastback rear end

$$Re = 4.87x10^6$$

83.74 million nodes

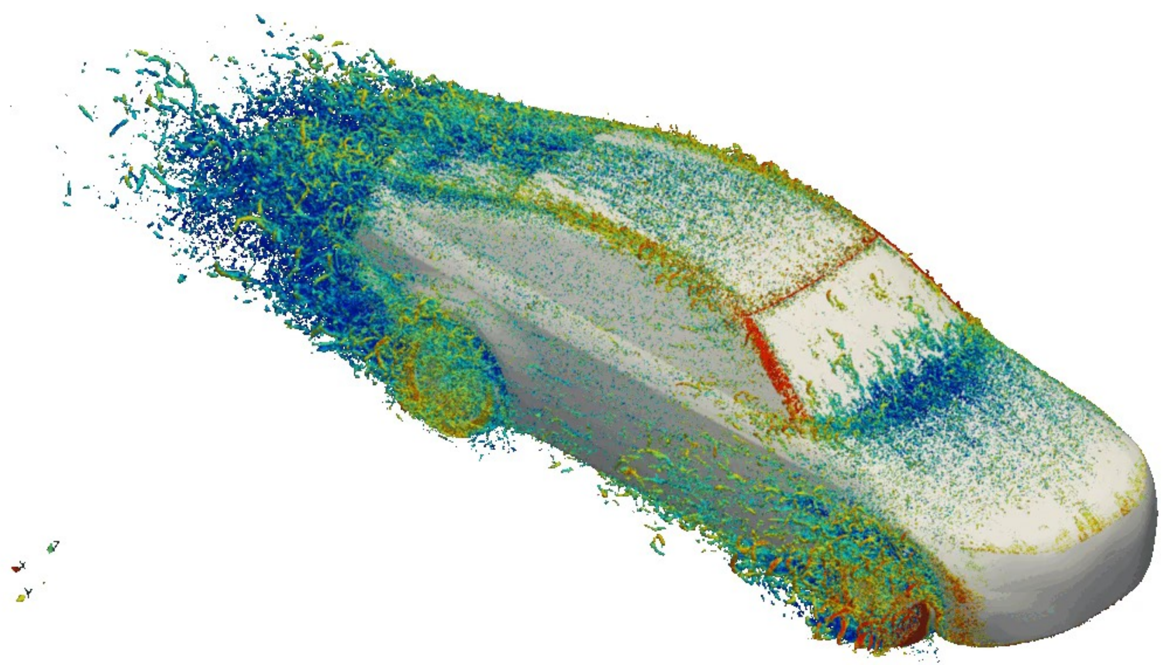

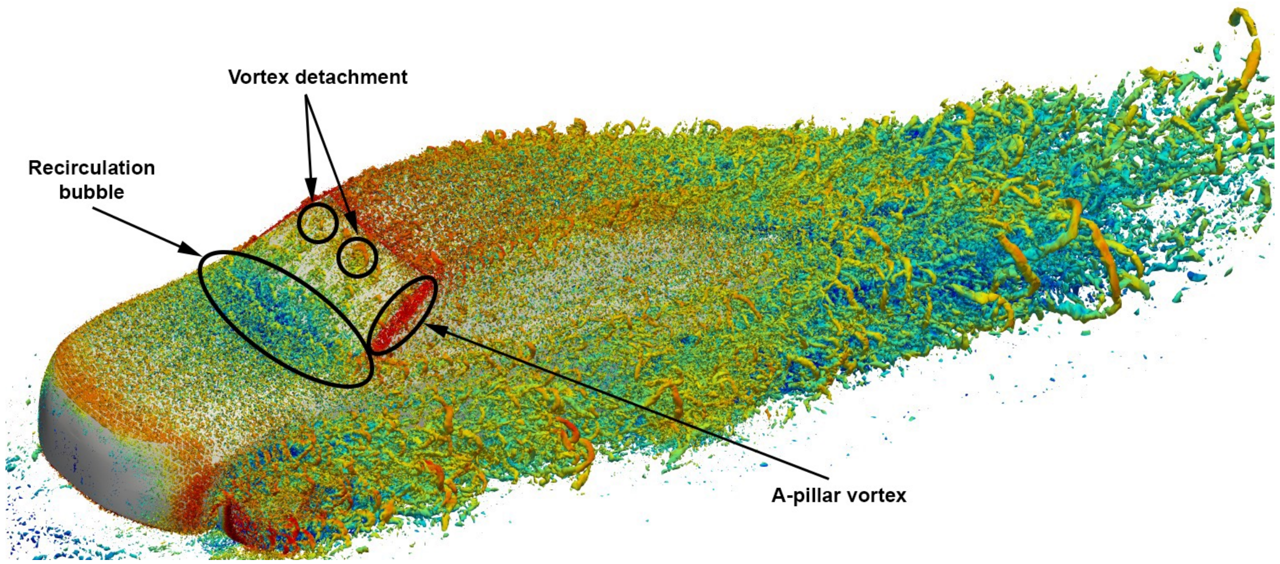

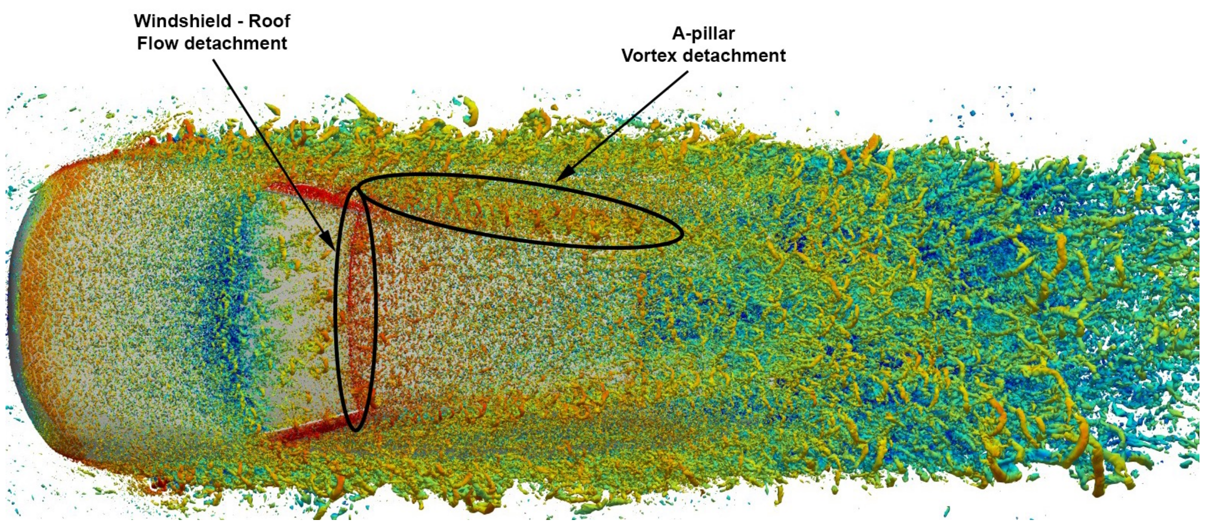

Validation: WMLES

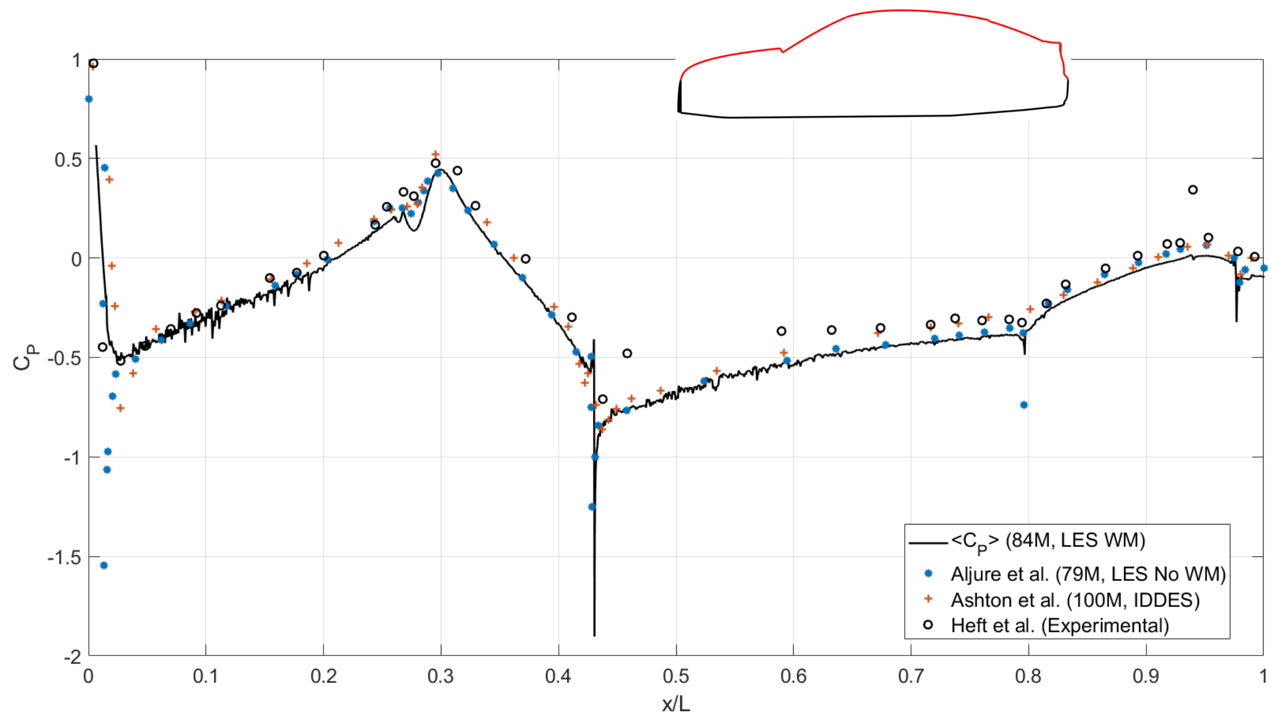

Case	Approach	$< C_D >$	$< C_D >$ Relative Error (%)
Present Work	LES	**0.234**	-
James et al. [1]	Experimental	0.230	1.739
Mack et al. [2]	Experimental	0.238	1.681
Heft et al. [3]	RANS	0.233	0.429
Heft et al. [4]	Experimental	0.242	3.306
Miao et al. [5]	Experimental	0.245	4.490

Results with smooth underbody, static ground simulation and without mirrors

[1] T. James, L. Krueger, M. Lentzen, S. Woodiga, K. Chalupa, B. Hupertz, N. Lewingtion (2018), doi: 10.4271/2018-01-0731
[2] S. Mack, T. Indinger, N. Adams, S. Blume, P. Unterlechner (2012), doi: 10.1115/fedsm2012-72371
[3] A. Heft, T. Indinger, N. Adams (2012), doi: 10.1115/fedsm2012-72272
[4] A. Heft, T. Indinger, N. Adams (2012), doi: 10.4271/2012-01-0168
[5] L. Miao, S. Mack, T. Indinger (2015), doi: 10.1115/detc2015-47805.

Validation: WMLES

Parallel performance on 4 GPU NVIDIA GeForce RTX 3090

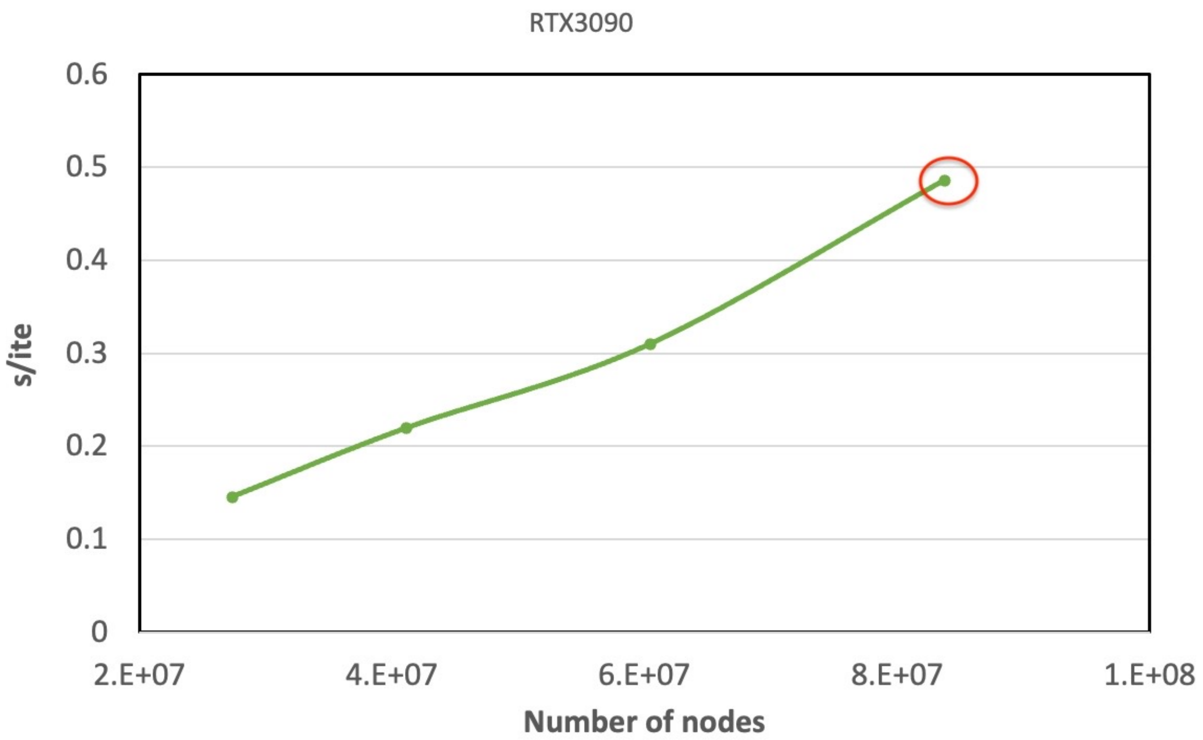

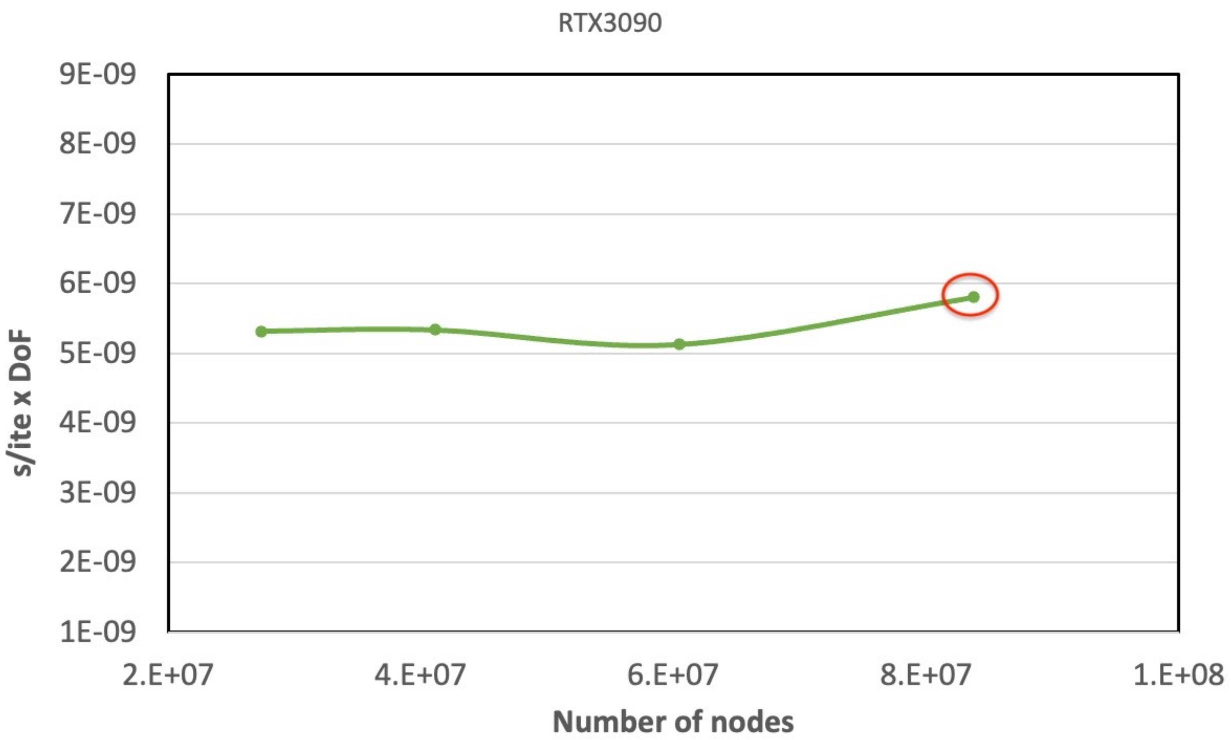

Server	N° CPU/GPU	Cost [€]	Mesh Nodes	Δt_{avg} [TU]	Wall Time [h]	s/iteration
Juno GPU	4	23 445	84 M	$2.421 \cdot 10^{-5}$	37	0.486
FinisTerrae CPU [1]	1024	231 500	79 M	$8.83 \cdot 10^{-6}$	264	1.1

[1] D. Aljure, J. Calafell, A. Baez, A. Oliva (2018), doi: 10.1016/j.jweia.2017.12.027

Outline

- ❑ Technical challenges for scale resolving applications
- ❑ Numerical approach - Low-dissipation schemes
- ❑ Applications: WRLES, flow control
- ❑ Data analysis: Reduced order models

Towards industrial applications for flow control

Flow control
Wall-resolved LES
SD7003 Re=6×10^4 AOA=4º, 11º, 14º

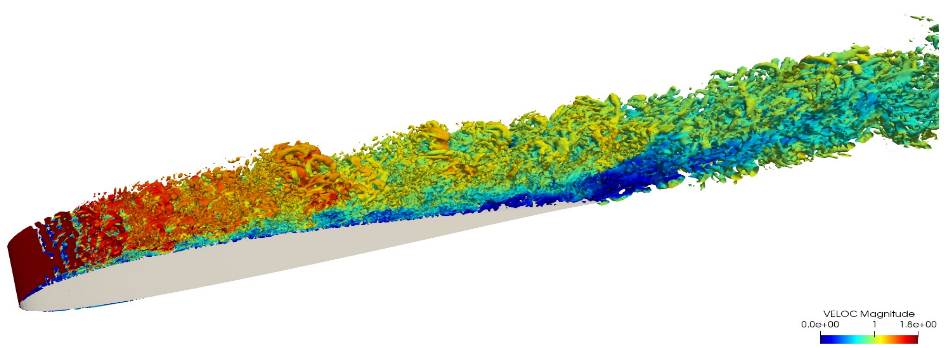

Flow control
Aircraft full-stall
WMLES
Re=1.93×10^6 AoA = 21.51º

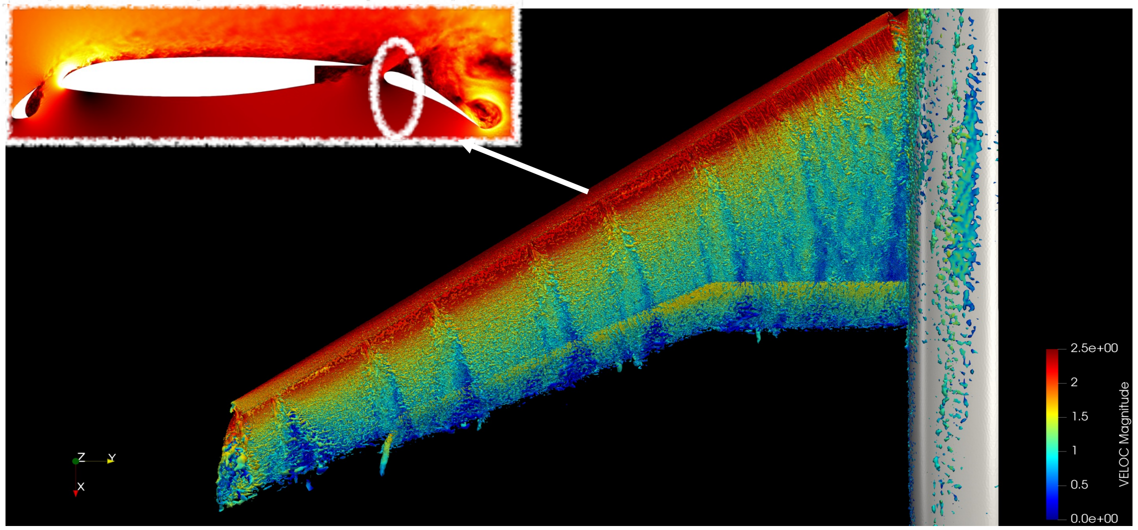

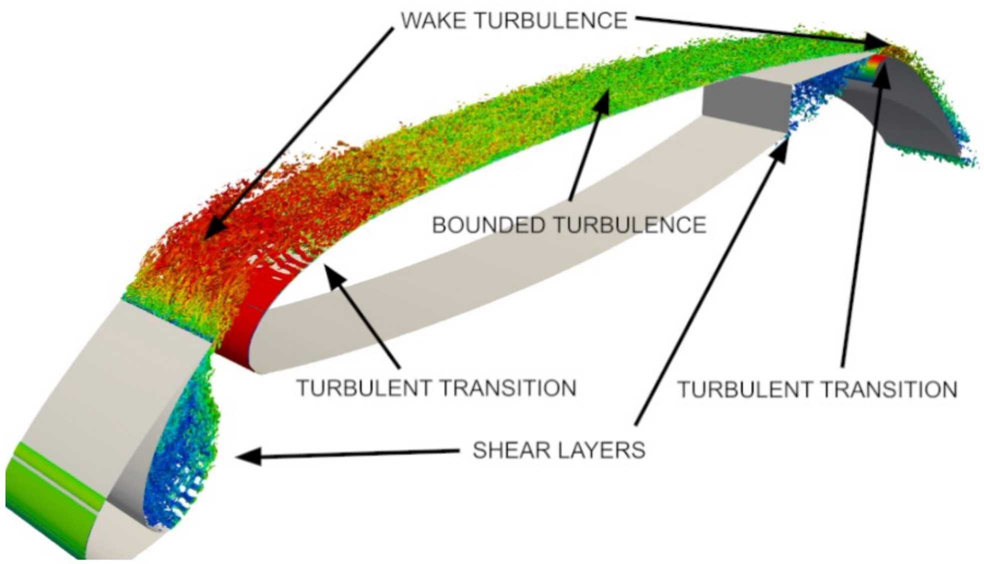

Wall-resolved LES
30p30n Re=7.5×10^5

Applications: AFC for separation

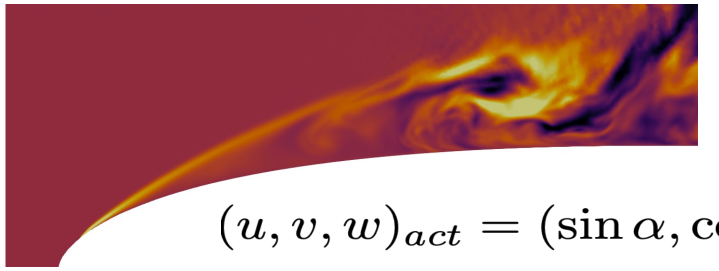

SD 7003 Re=60000

$$(u, v, w)_{act} = (\sin\alpha, \cos\alpha, 0) A_p \sin(2\pi f t) U_{ref} \sin(2\pi\tau z)$$

$$U_{max} = A_p U_{ref}$$

$$F^+ = f U_{ref} / x_{TE}$$

$$c_\mu = h(\rho U_{max}^2)/(C \rho U_{ref}^2)$$

Location	0.007
F^+	1
C_μ	**0.003**, 0.006

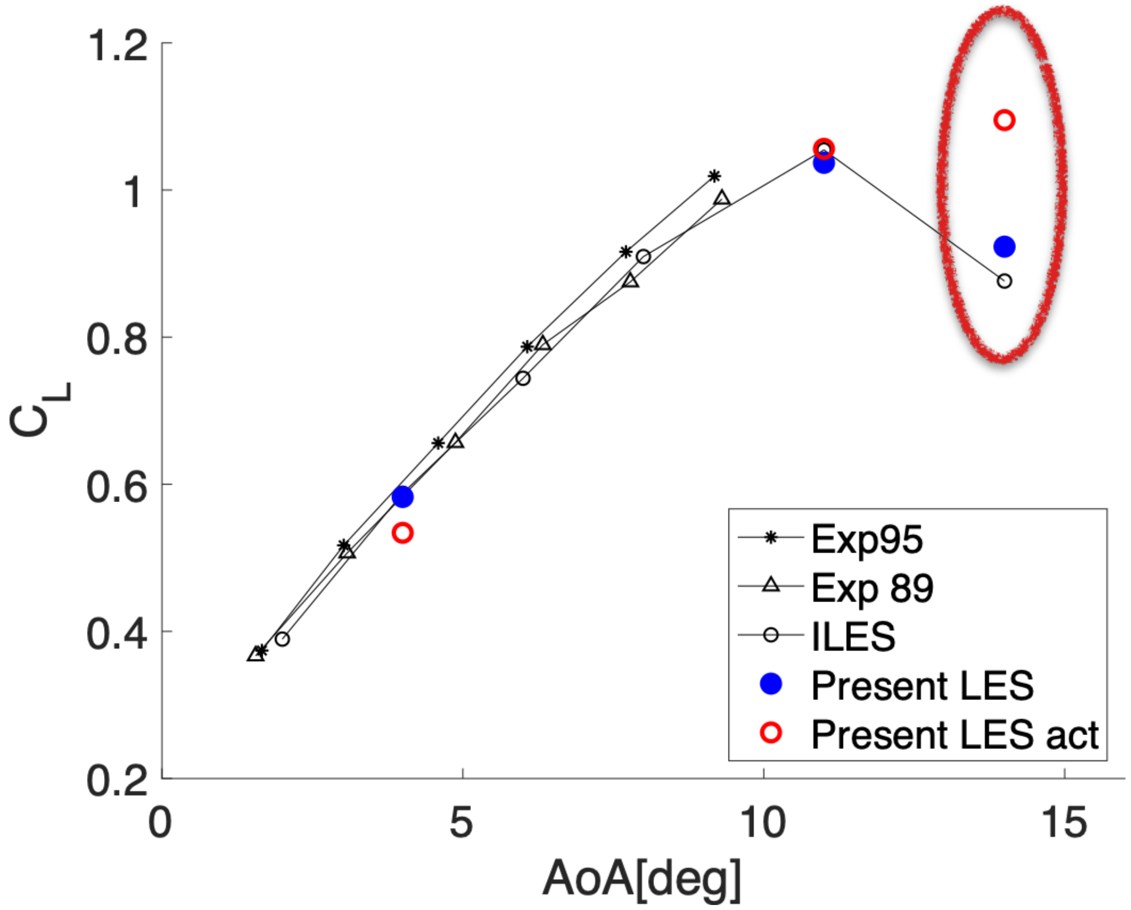

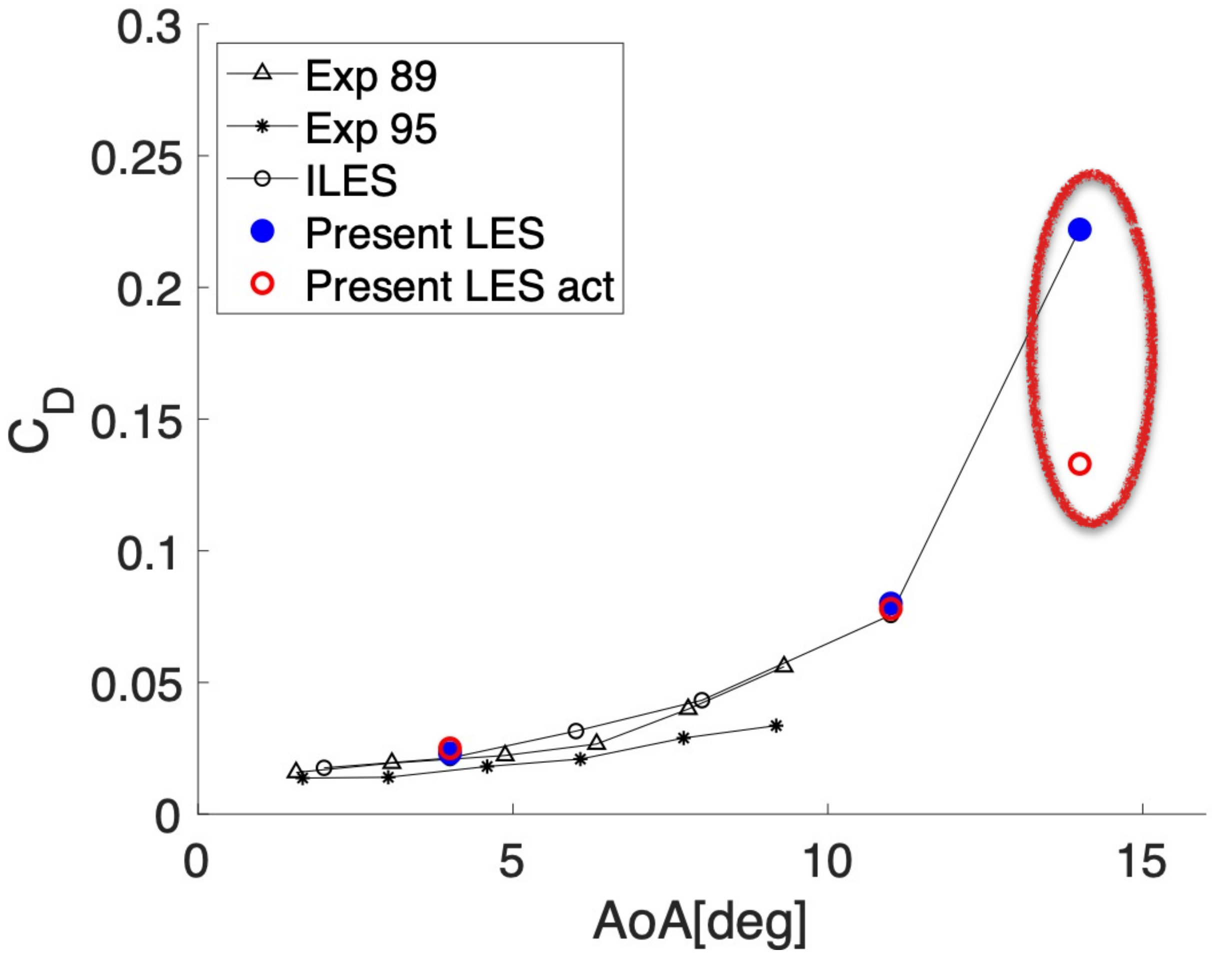

Applications: AFC for separation

AOA=14º

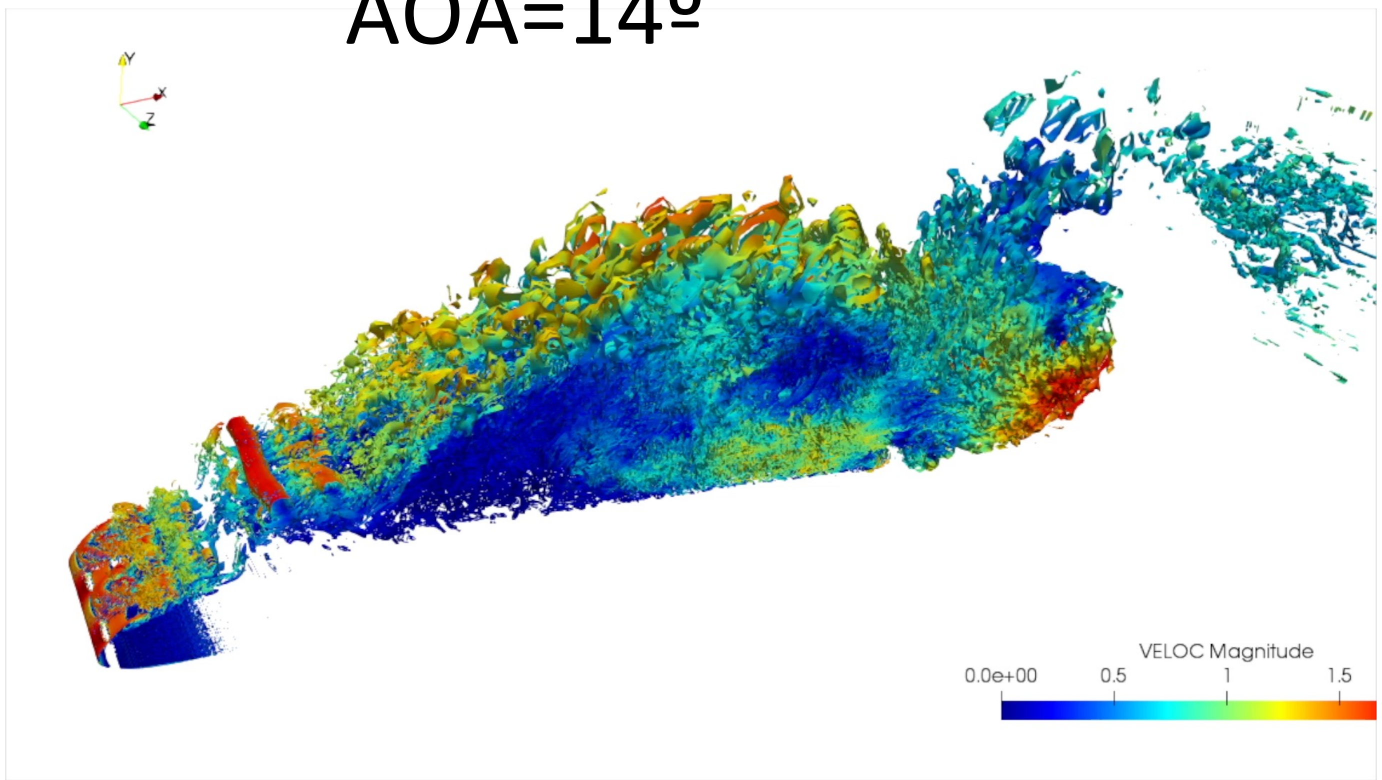

$$C_L^{baseline} = 0.88\ vs.\ C_L^{actuated} = 1.101\ (+24\%)$$

$$C_D^{baseline} = 0.24\ vs.\ C_D^{actuated} = 0.13\ \ (-52\%)$$

Aerodynamic efficiency increases by 124%

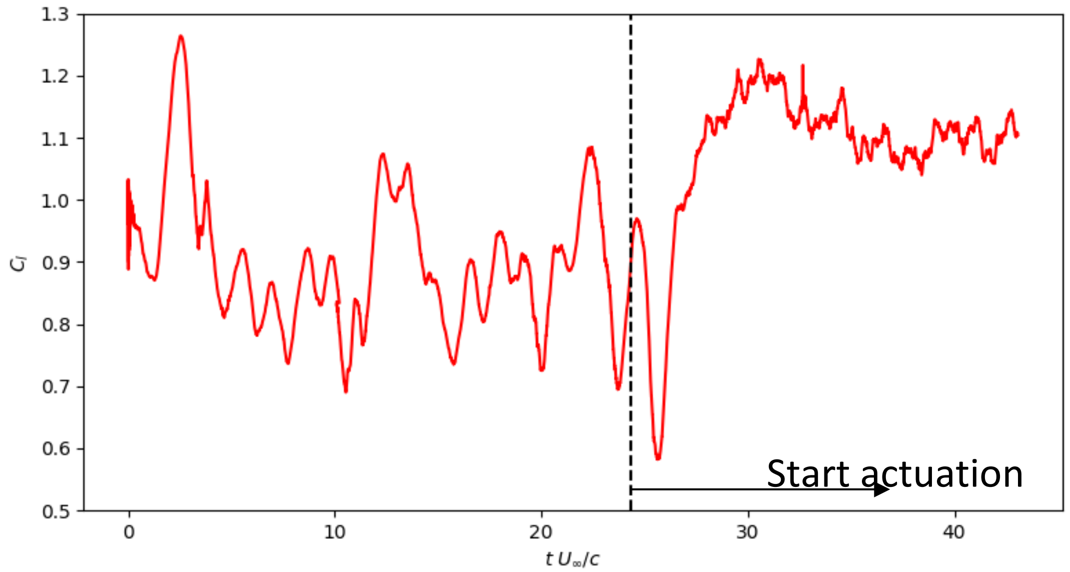

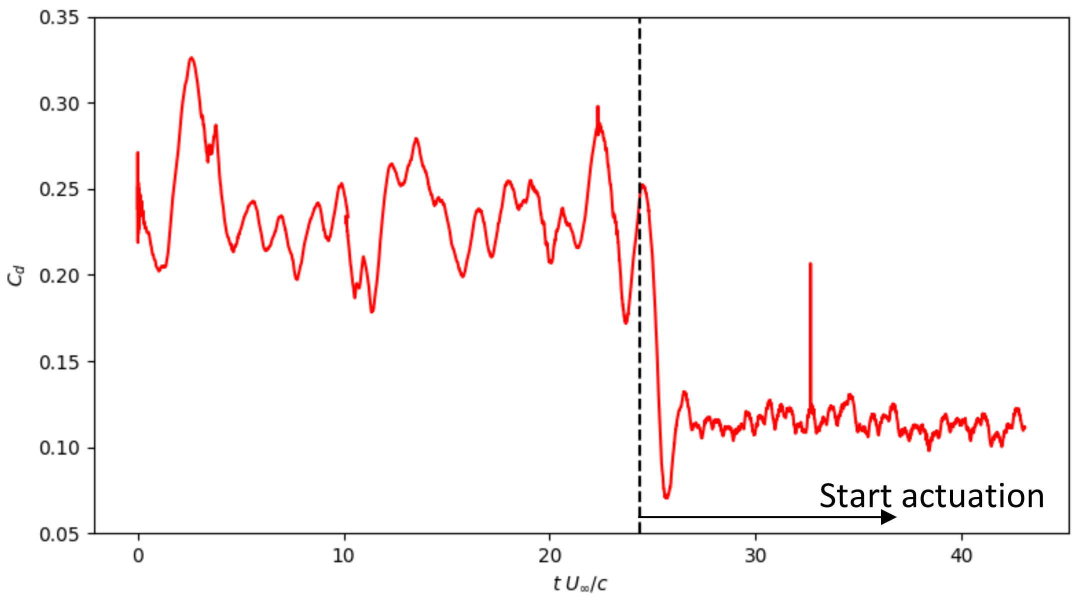

- The actuation succeeded at suppressing the LSB, but no improvement in aerodynamic efficiency at AoA < CLmax
- CL increases and Cd decreases at high AoA

Its possible to control massive separation

JAXA high-lift Re=1.93×10^6 AOA = 21.51º

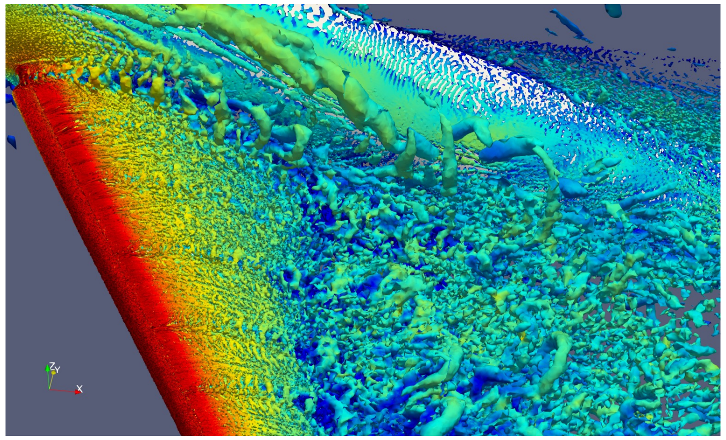

How does the actuation perform on a three-dimensional turbulent BL?

- AFC in both main and flap
- Wall-modelled LES - 65 M grid-points

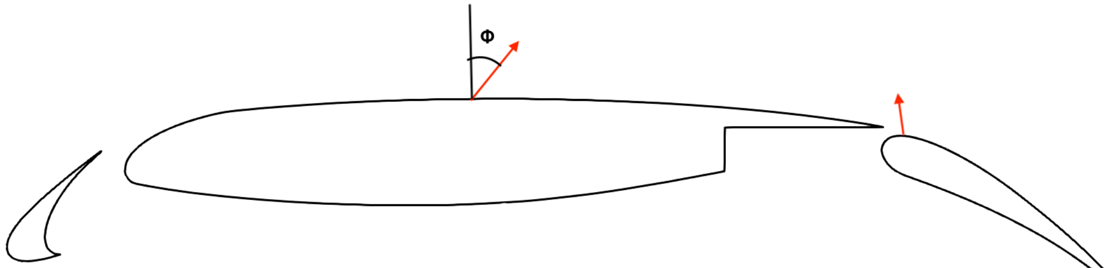

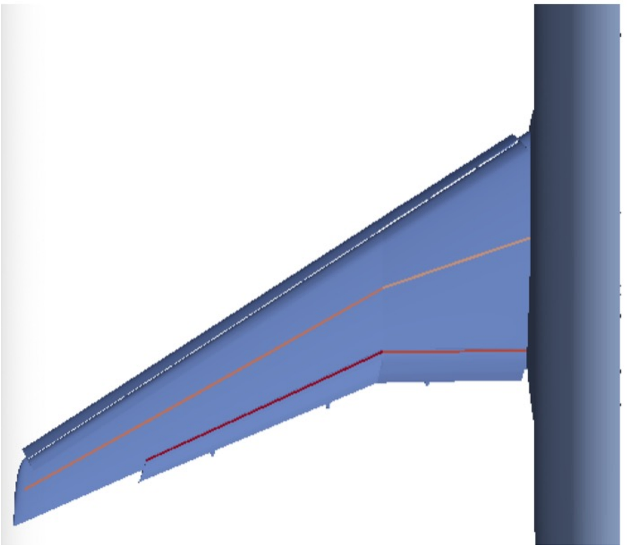

$$(u, v, w)_{act} = V_{max} \sin(2\pi f t) \cos(2\pi \tau_y y)(\cos\alpha, sin\alpha, 1)(\sin\Phi, \sin\Phi, \cos\Phi)$$

$$C_\mu = 0.15 - 1.5\% \quad \Phi = 0 - 45^\circ \quad F^+ = 1.52 \quad \tau_y = 0.1$$

Applications: AFC of an aircraft in full stall

Summary of the cases

Case		Φ[deg]	C_μ	F^+	3D/2D
AFC1	Main	0	0.015	1.52	3D
	Flap	0			
AFC2	Main	-	-	-	-
	Flap	0	0.015	1.52	3D
AFC3	Main	0	0.015	1.52	3D
	Flap	0	0.0015		
AFC4	Main	-	-	-	-
	Flap	0	0.0015	1.52	3D
AFC5	Main	60	0.0075	1.52	2D
	Flap	0	0.0015		3D
AFC6	Main	60	0.015	1.52	2D
	Flap	0	0.0015		3D
AFC7	Main	60	0.0075	1.52	3D
	Flap	0	0.0015		
AFC8	Main	45	0.015	1.52	2D
	Flap	0	0.0015		3D
AFC9	Main	45	0.015	15.2	2D
	Flap	0	0.0015		3D
AFC10	Main	45	0.015/0.023	1.52	2D
	Flap	0	0.0015		3D

Applications: AFC of an aircraft in full stall

Only flap actuation

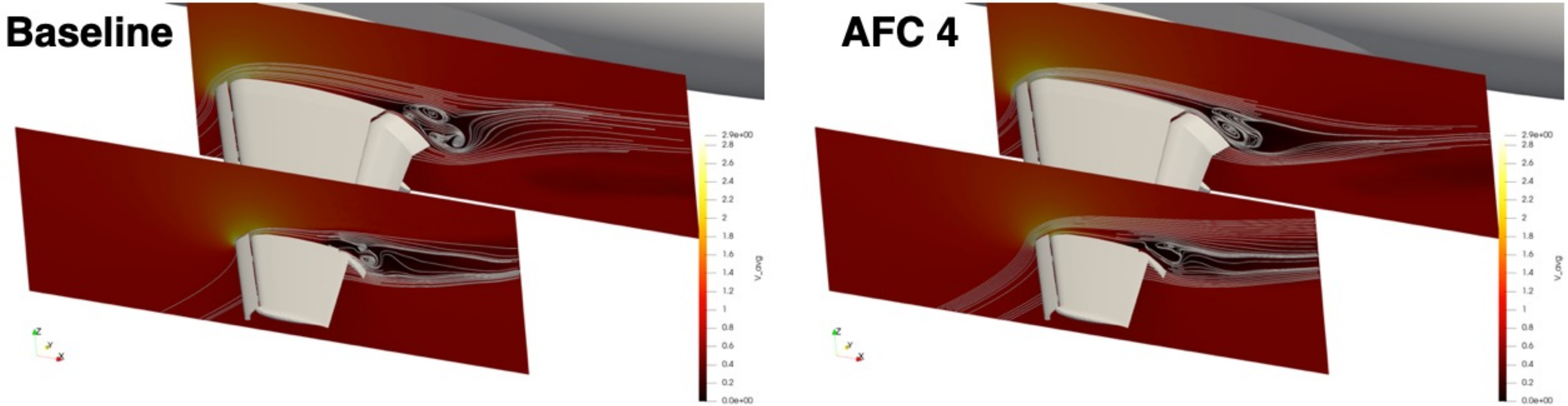

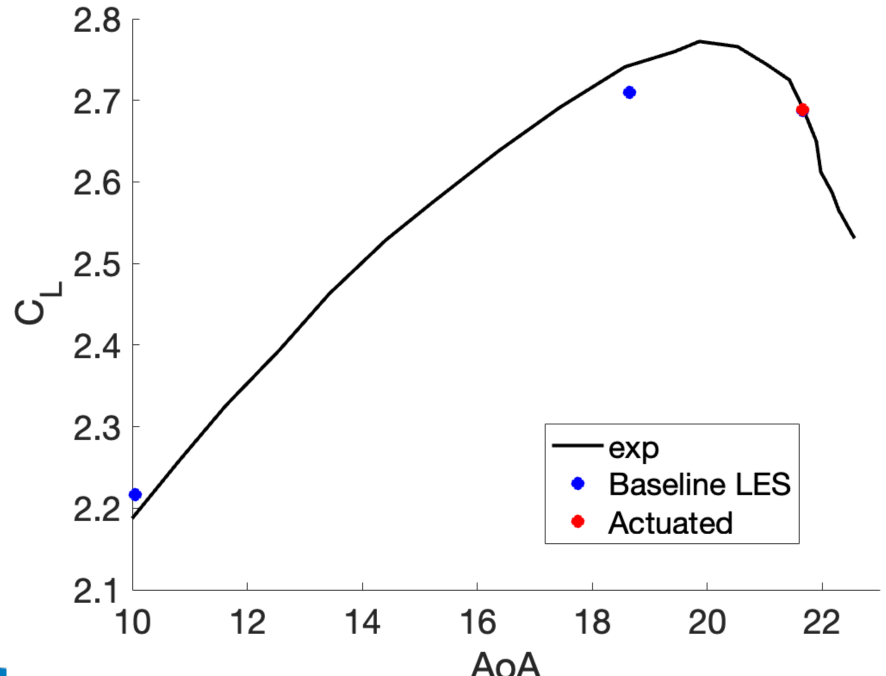

	C_L	C_D	C_L/C_D	C_{Lrms}	C_{Drms}
Baseline	2.685	0.405	6.630	0.004	0.002
AFC4	2.689(0.1%)	0.380 (6.2%)	7.080 (6.8%)	0.012	0.005

Applications: AFC of an aircraft in full stall

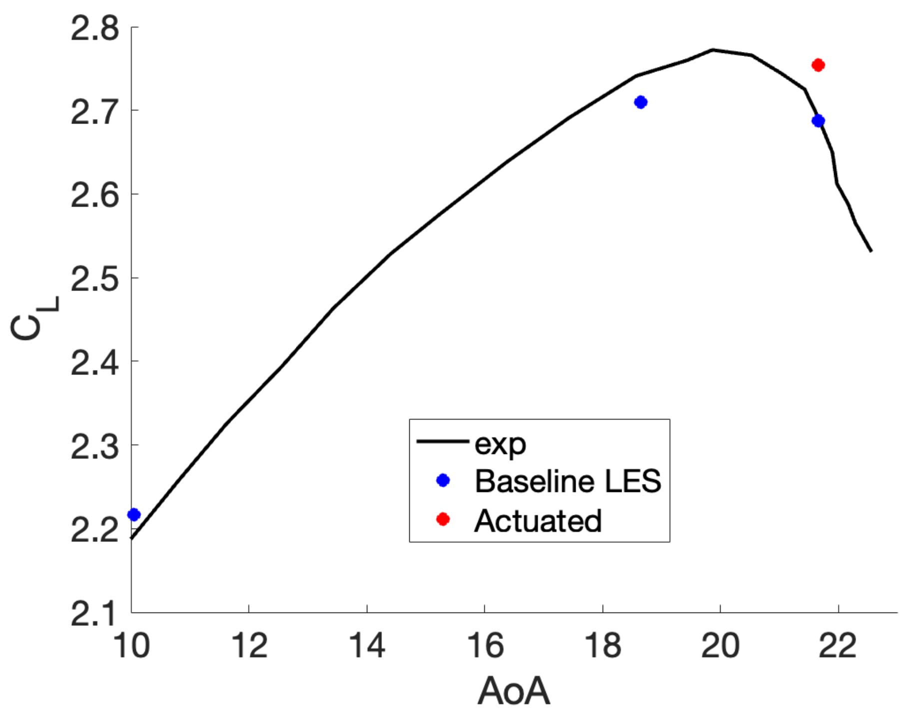

Maximum C_L

	C_L	C_D	C_L/C_D
Baseline	2.685	0.405	6.630
AFC10	**2.754(2.6%)**	0.391 (3.5%)	7.040 (6.2%)

Baseline

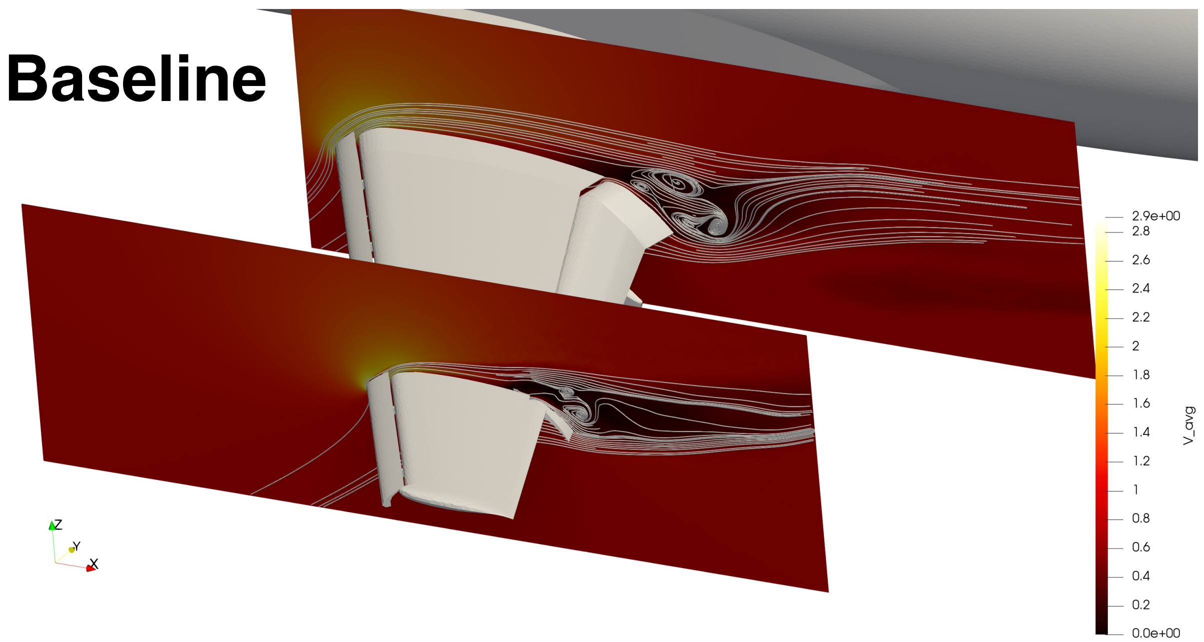

AFC 10

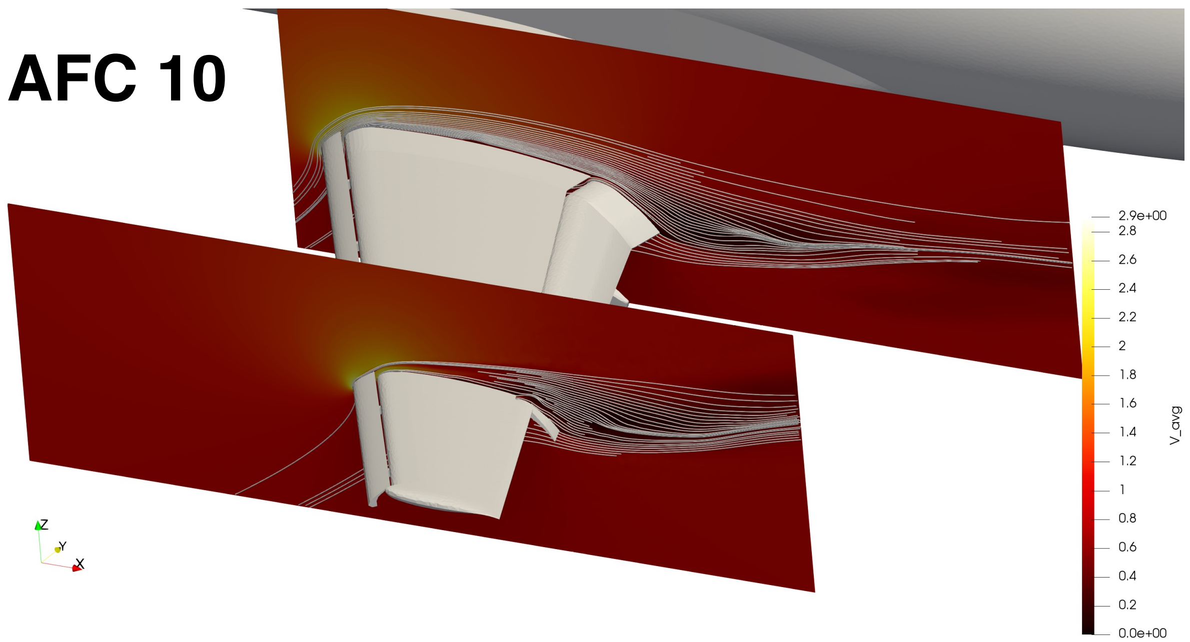

Applications: AFC of an aircraft in full stall

	C_L	C_D	C_L/C_D
Baseline	2.685	0.405	6.630
AFC10	**2.754(2.6%)**	0.391 (3.5%)	7.040 (6.2%)

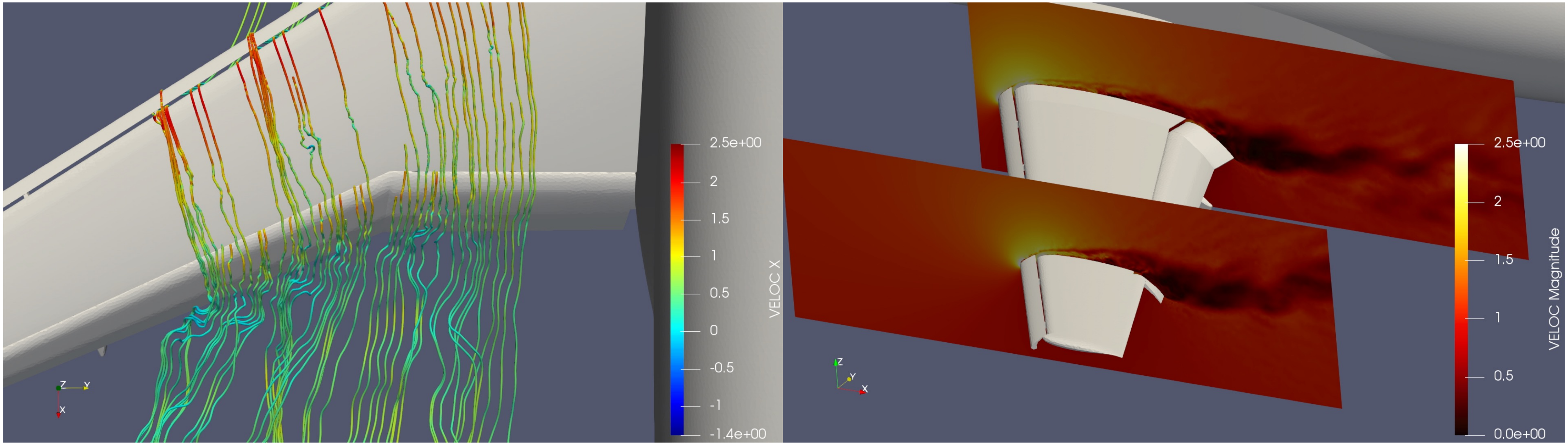

Lessons learned: It is possible to control a 3D wing but optimum parameters are yet unknown

Application: WRLES - 30p30n $Re=7.5x10^5$

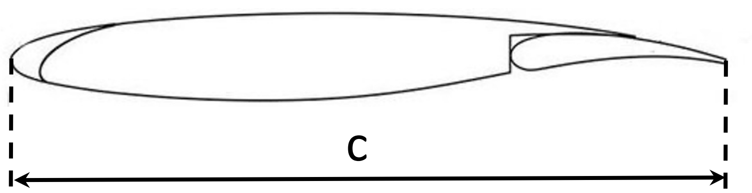

$$Re_c = \frac{\rho U_\infty c}{\mu}$$

Q-criterion Iso-contours at α=5º

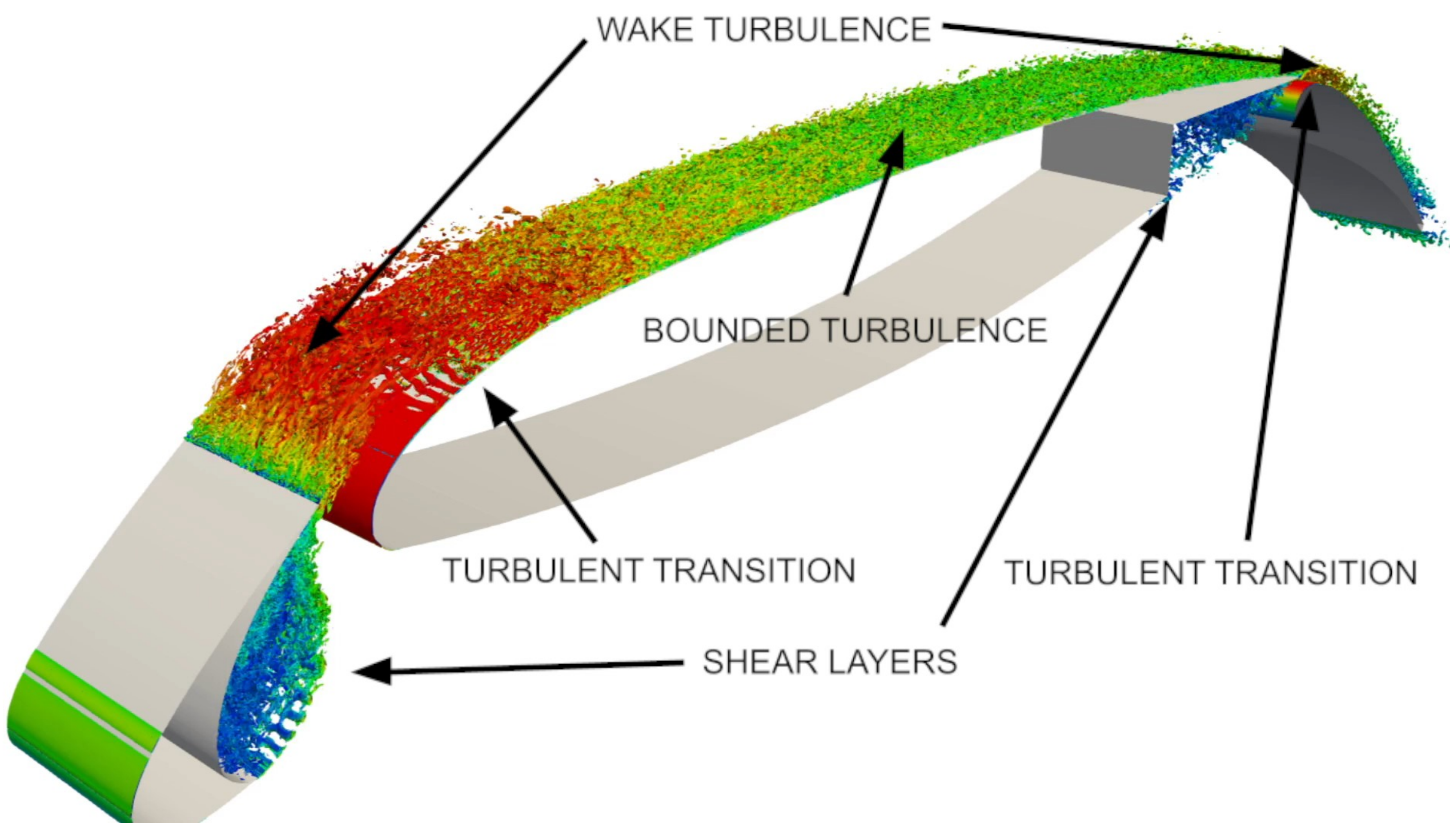

Applications: 30p30n Re=7.5x10^5

Pressure Coefficient (C_p)

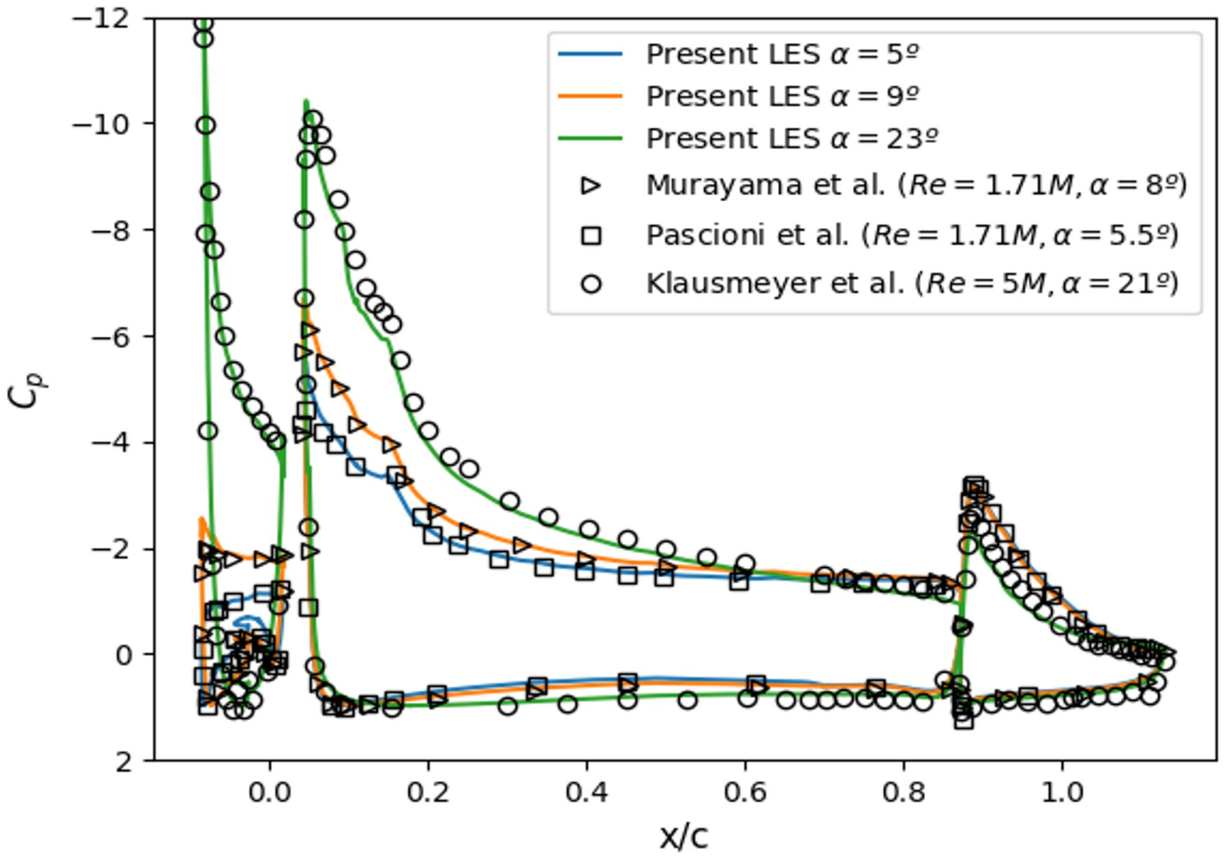

Skin Friction Coefficient(C_f)

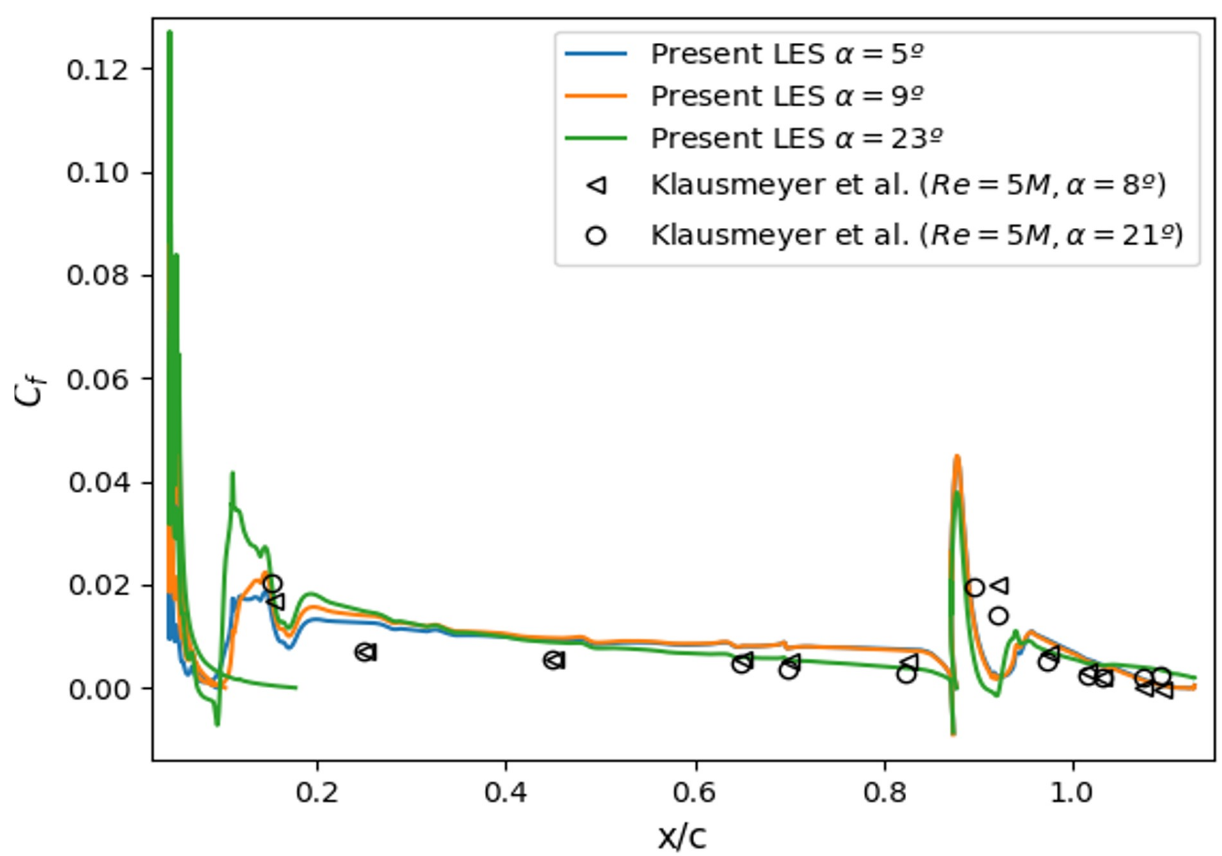

[6] M. Murayama, K. Nakakita, K. Yamamoto, H. Ura, Y. Ito, M. Choudhari (2014). DOI: https://doi.org/10.2514/6.2018-3460

[7] K. Pascioni, L.N. Cattafesta, M. Choudhari (2014). DOI: https://doi.org/10.2514/6.2014-3062

[8] S. Klausmeyer, J. Lin (1994). DOI: https://doi.org/10.2514/6.1994-1870

Applications: 30p30n Re=7.5x10^5

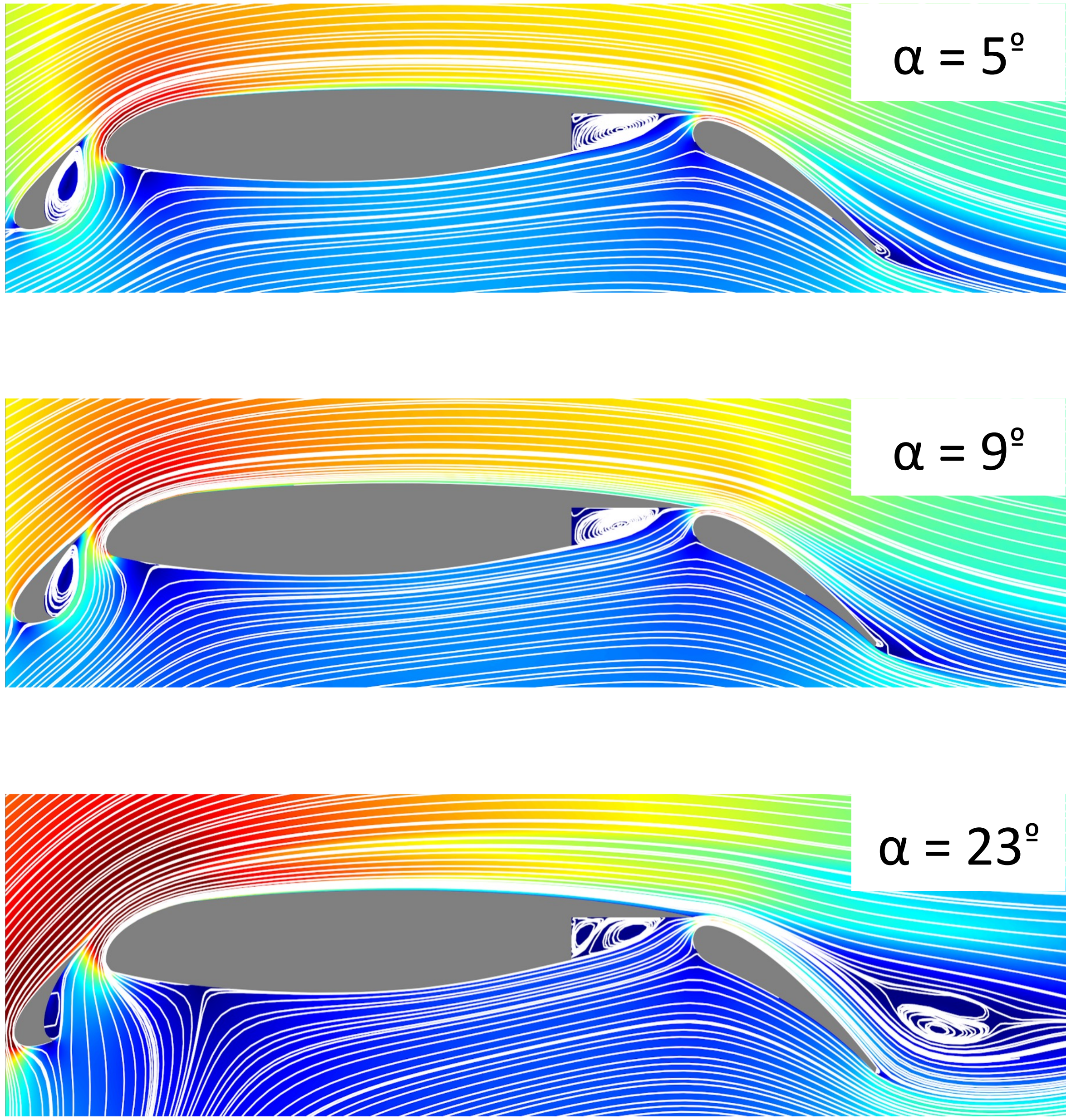

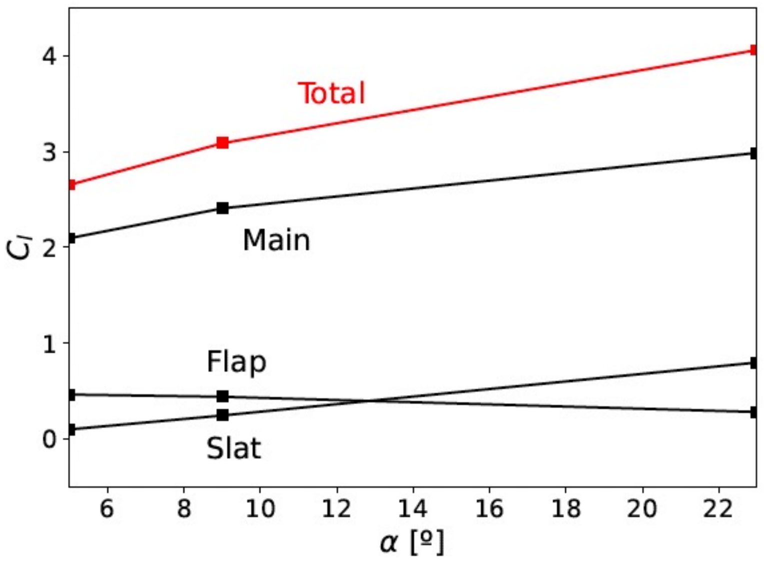

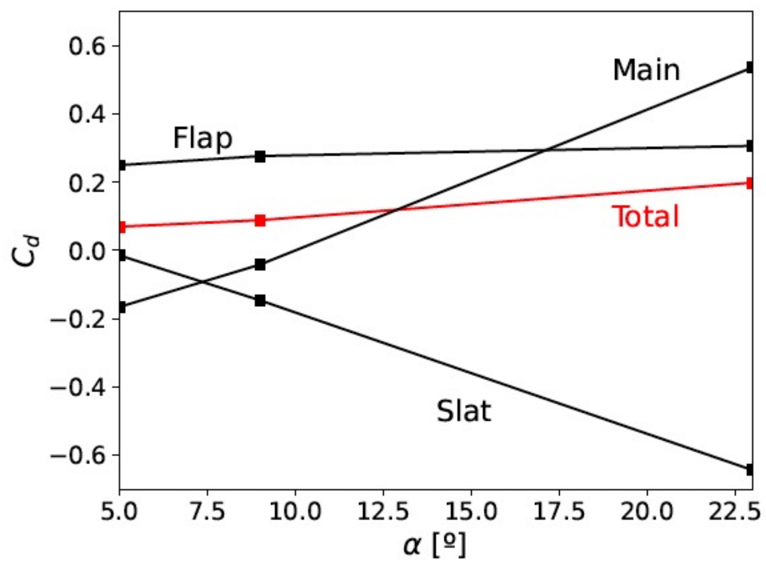

- Large contribution of the flap
- Effect of the wake
- Recirculation

Applications: 30p30n Re=7.5x10^5

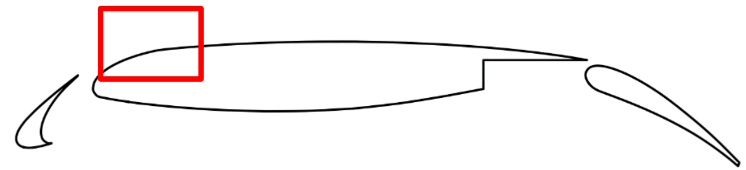

α = 5º | α = 9º | α = 23º

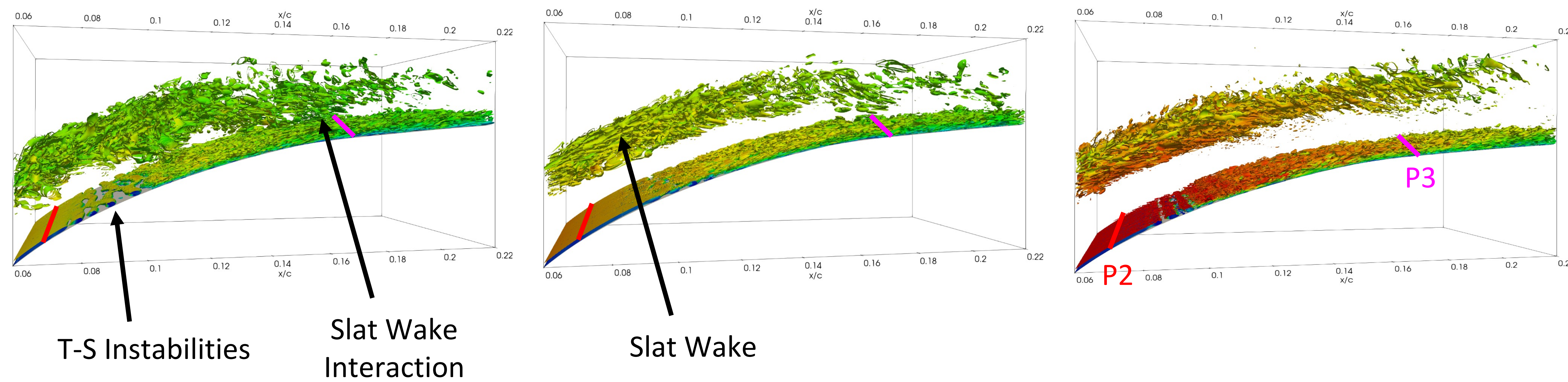

Velocity Magnitude Spectra at P2

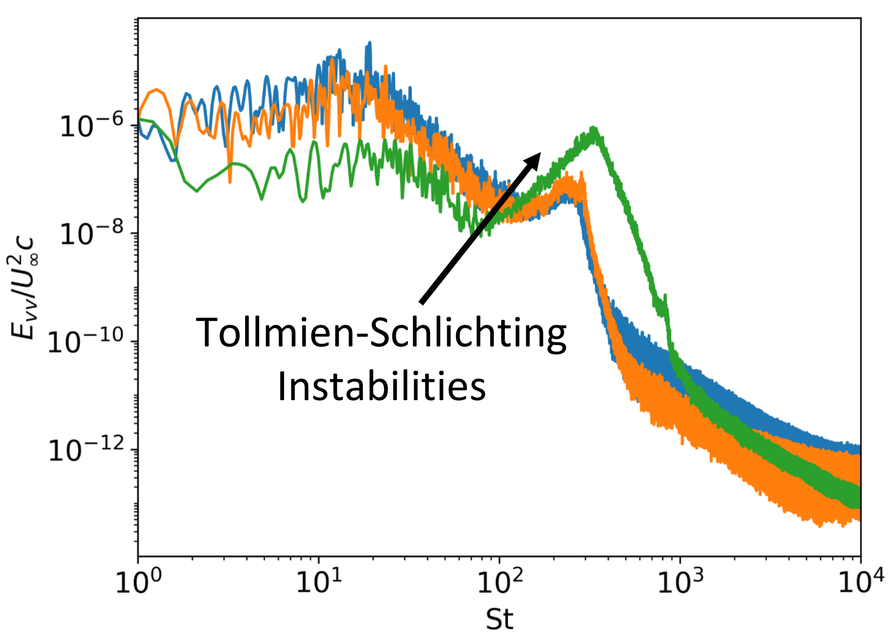

α [º]	St [-]
5	255
9	285
23	340

Skin Friction Coefficient

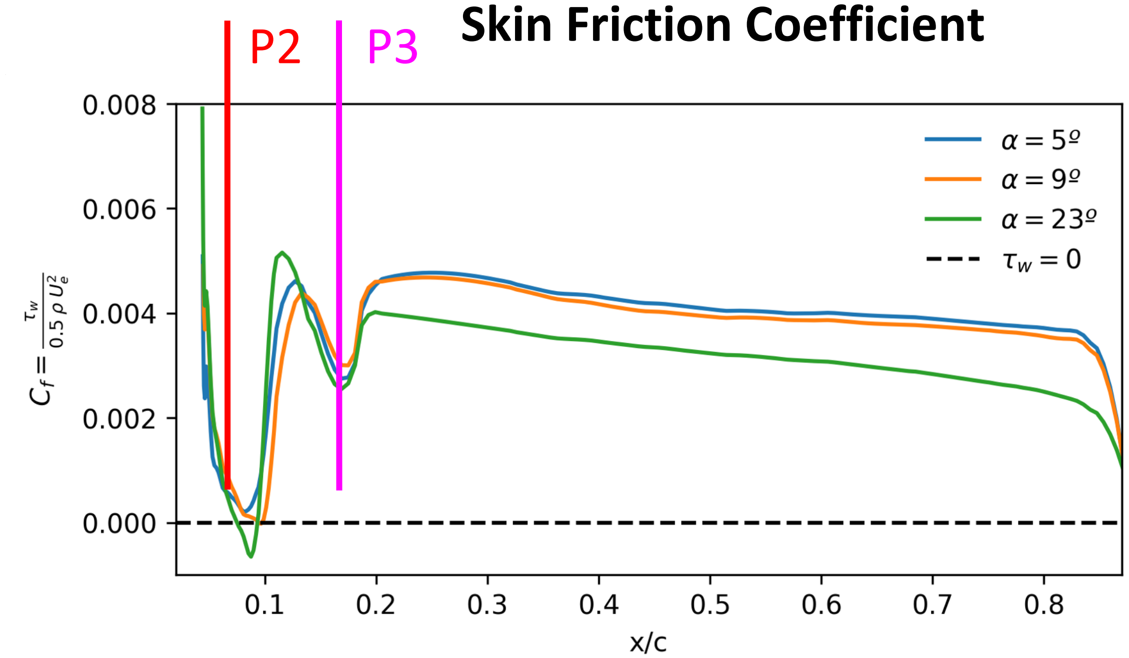

Applications: 30p30n Re=7.5×10^5

Lessons learned:

What's the best strategy to control the flow?

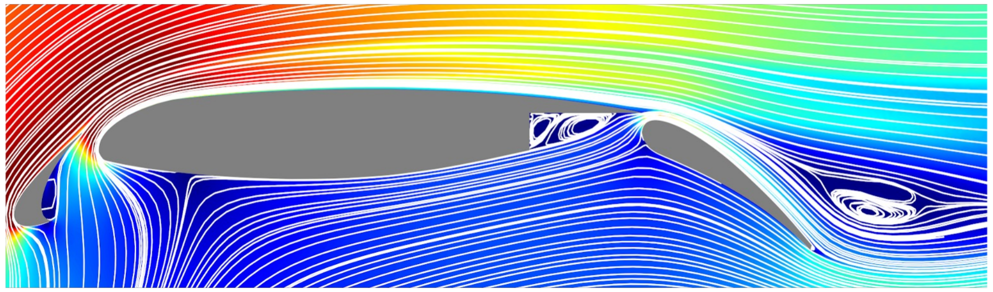

Reduce the wakes produced by the slat and main elements -> placing the jets on the slat surface with the aim to bring the slat wake closer to the main wall could potentially reduce the APG and thus enhance the wing efficiency.

Separation of the slat wake from the main surface contributes to strengthening the APG.

Multitude of parameters involved, addressing this issue through conventional parametric studies seems challenging. Therefore, given the advancements in artificial intelligence (AI), **integrating AFC with deep reinforcement learning (DRL)** emerges as a compelling approach

Next target: Can we discover new actuation strategies through DRL?

Applications: DRL-based AFC

- $Re = 100$
- $N_{dofs} = 3.27M$
- **Mulit-agent Reinforcement Learning (MARL)** → 10 MARL pseudo-environments

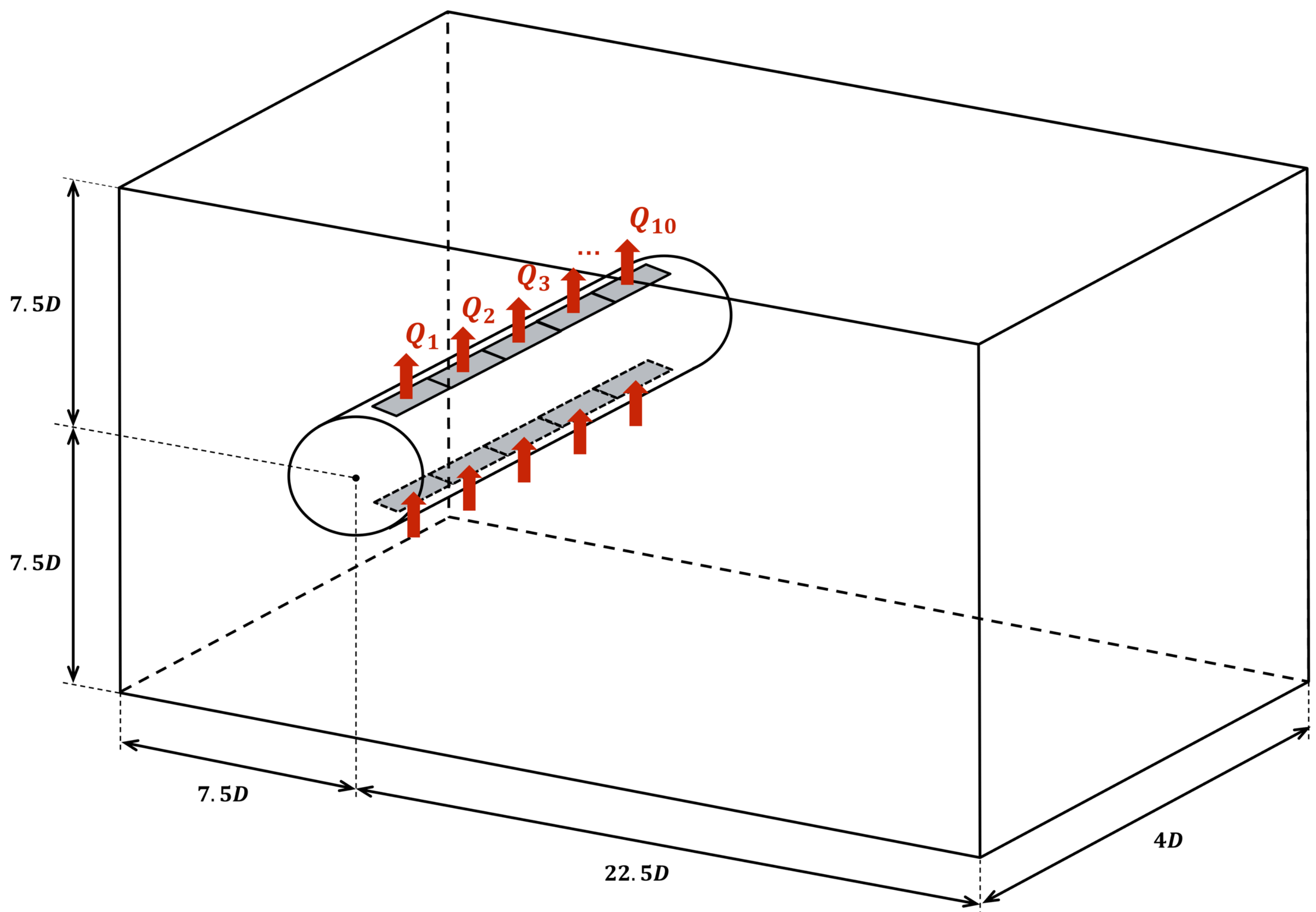

- **State in each pseudo-environment:**

Pressure at 85 x 3 slices = 255 points

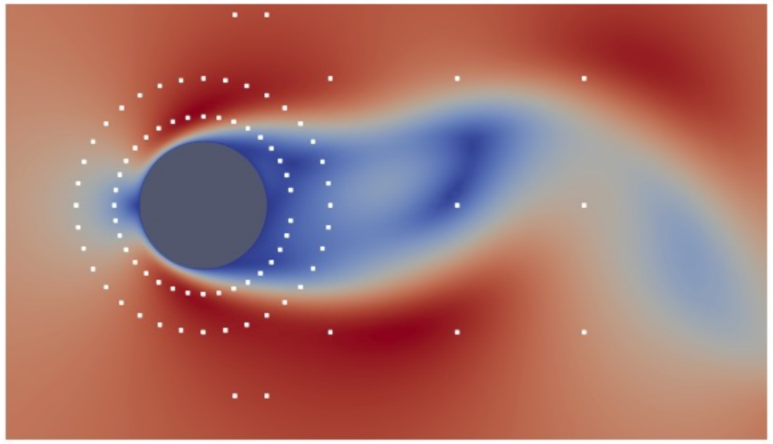

Local contr. Global contr.

$$R_i = \beta r_i + (1-\beta)\sum_{j=1}^{10} r_j/10$$

$$r_i = C_{d,baseline} - C_{d,i} - \alpha|C_{l,i}|$$

Drag contr. Lift contr.

β (Local Weight)	0.8
α (Lift Penalty)	0.3

Applications: DRL-based AFC

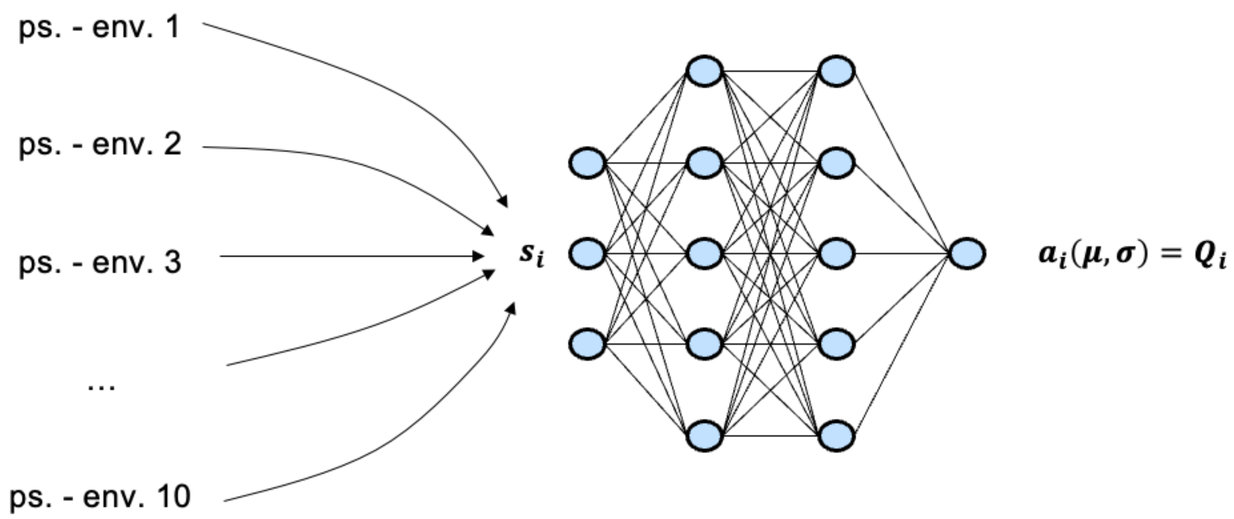

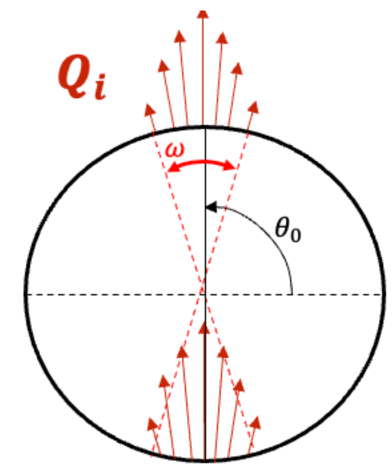

$$|U_i(Q_i, \theta)| = Q_i \frac{\pi}{\rho D \omega} \cos\left(\frac{\pi}{\omega}(\theta - \theta_0)\right)$$

ω	10º
θ_0	90º / 270

	#Neurons (layers)	512 (2)
Training	**Optimization algorithm**	Proximal Policy Optimization
	Number of episodes	50
	Number of MARL episodes	2000
	Episode duration	35 TU (6 vortex shedding)
	Action duration	0.29 TU (120 actions/episode)

4 CFD simulations x 10 MARL environments = 40

40 MARL environments x 50 episodes = 2000

Applications: DRL-based AFC

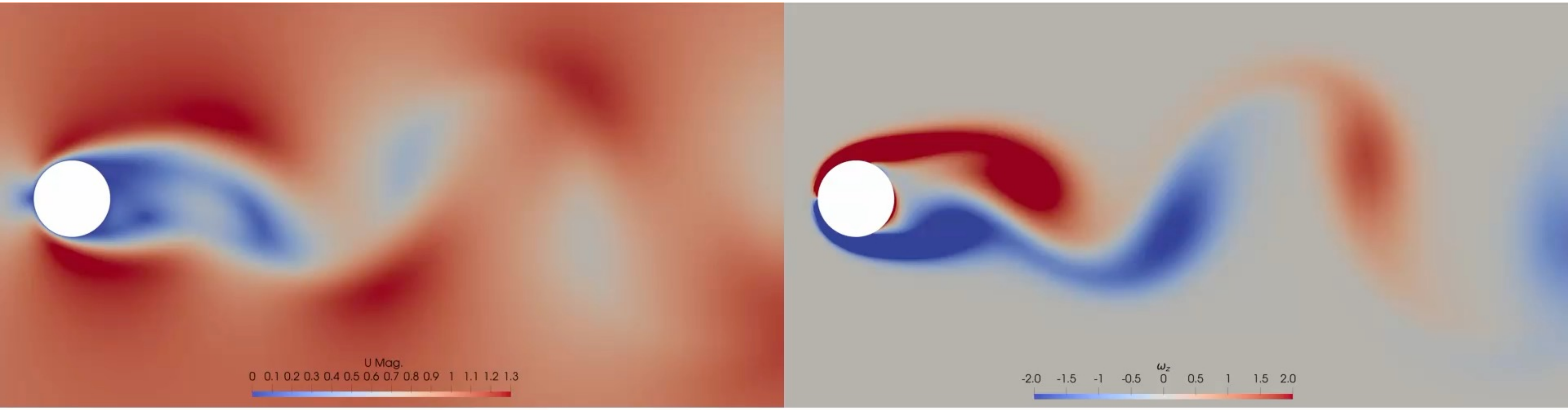

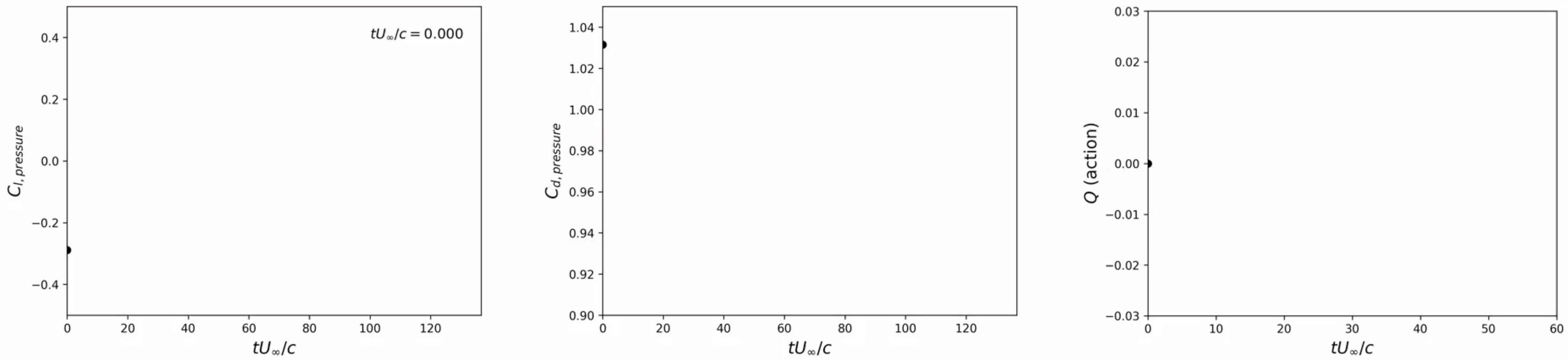

Applications: DRL-based AFC

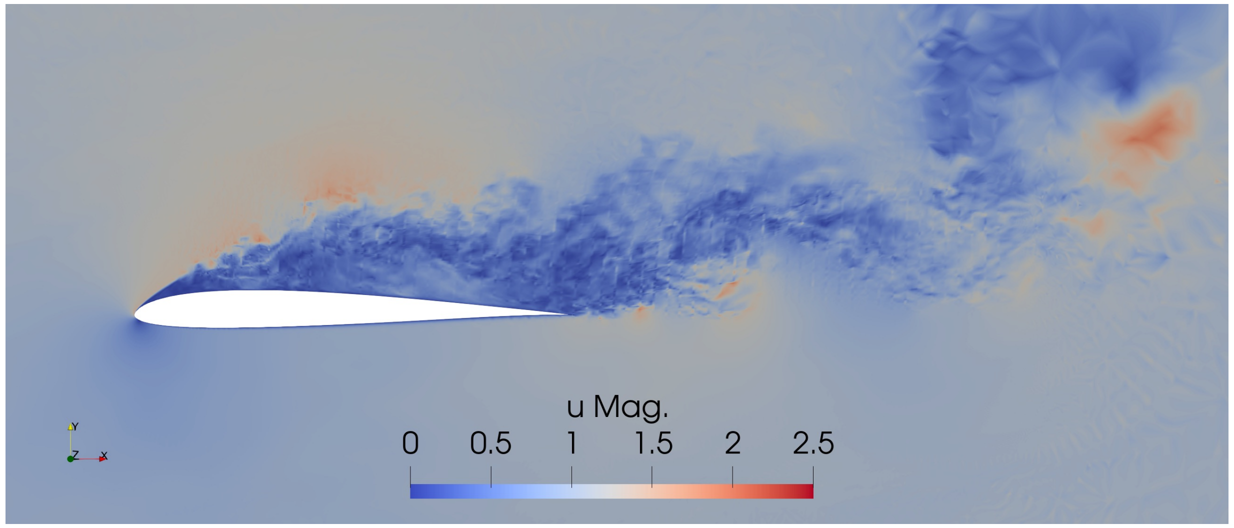

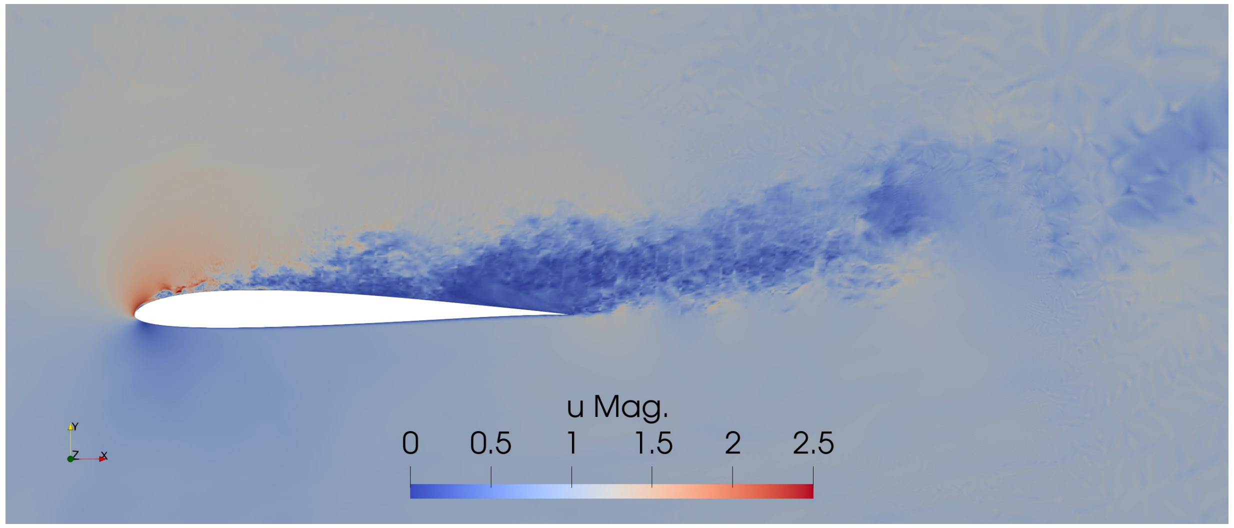

Solver	SOD2D (SEM)
Re	60,000
AoA	14º
N_{dofs} (order)	5M (p = 4)
N *training cycles*	4
N *episodes*	1000
N pseudo env	16
Target	Frequency, Cμ, position

Outline

- ❑ Technical challenges for scale resolving applications
- ❑ Numerical approach
  - Low-dissipation schemes
  - The wall problem: WMLES
- ❑ Applications: WRLES, flow control
- ❑ Data analysis: Reduced order models

Data analysis: Deep Learning Surrogate Models

Windsor body at $Re_L = U_\infty L/\nu = 2.9 \times 10^6$

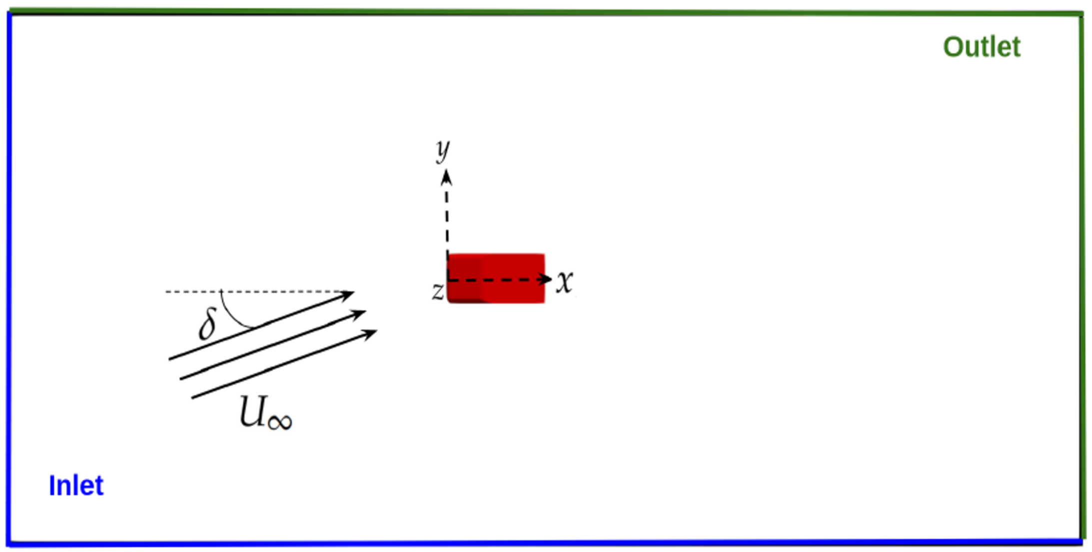

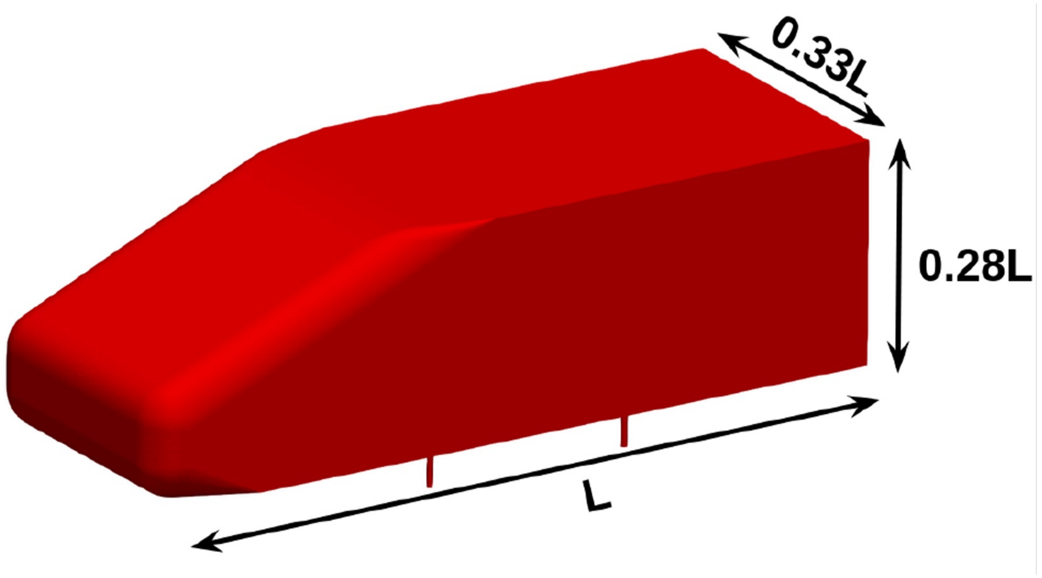

α = 2.5º

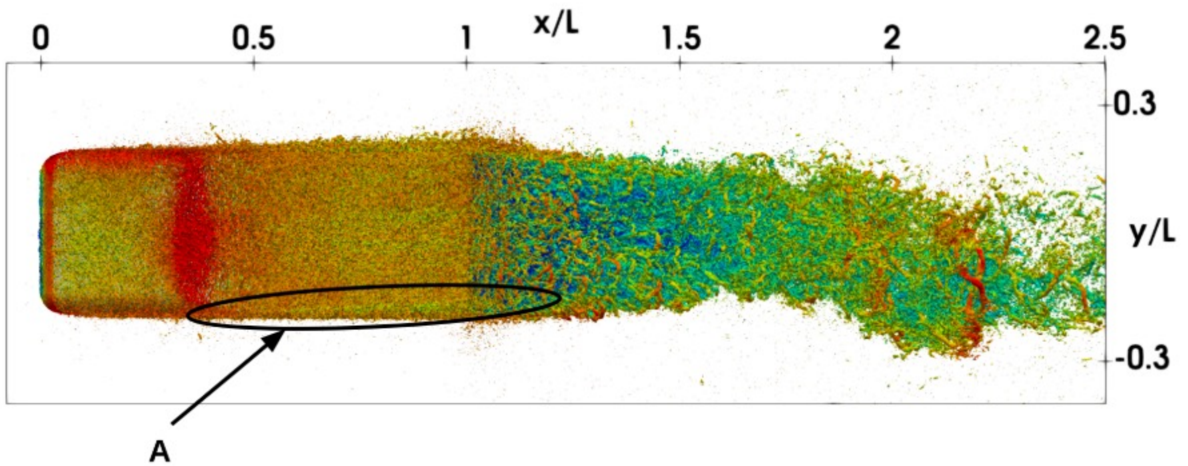

α = 10º

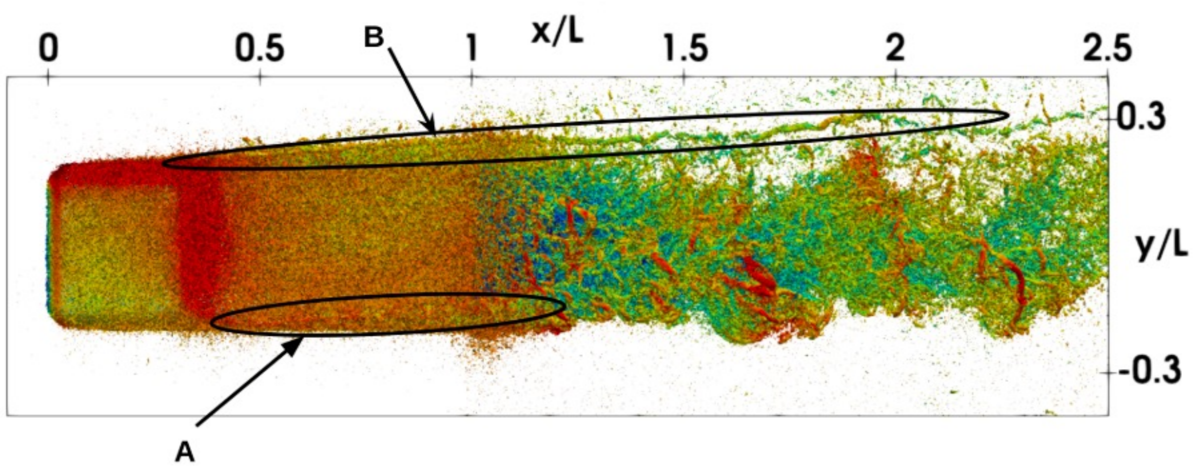

B. Eiximeno, A. Miró, I. Rodríguez, and O. Lehmkuhl, "*Mathematics*, vol. 12, no. 7, pp. 1–23, 2024.

Data analysis: Deep Learning Surrogate Models

Windsor body at $Re_L = U_\infty L/\nu = 2.9 \times 10^6$

The back pressure of a car is highly influenced by the yaw angle. The higher the yaw angle, the greater the suction and the drag force

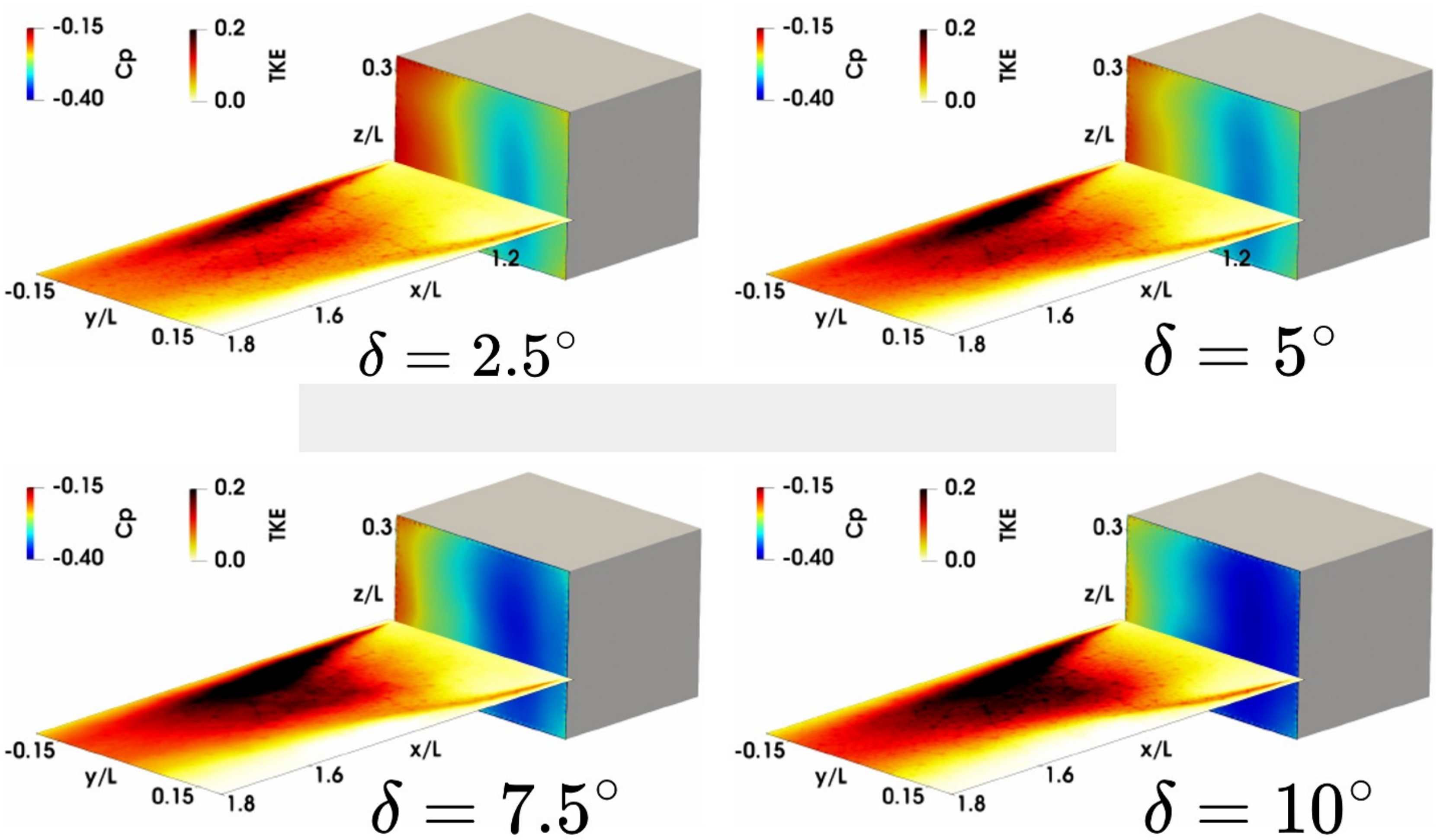

B. Eiximeno, A. Miró, I. Rodríguez, and O. Lehmkuhl, "*Mathematics*, vol. 12, no. 7, pp. 1–23, 2024.

Windsor body at $Re_L = U_\infty L/\nu = 2.9 \times 10^6$

- A CNN variational autoencoder has been trained with the back pressure
- 80% of the total 1980 collected snapshots for δ = [2.5º, 5º and 10º] have been used to train the autoencoder, while the remaining 20% were reserved as a validation set to assess possible overfitting of the model to the seen data.
- Two latent vectors were enough to recover the original dataset

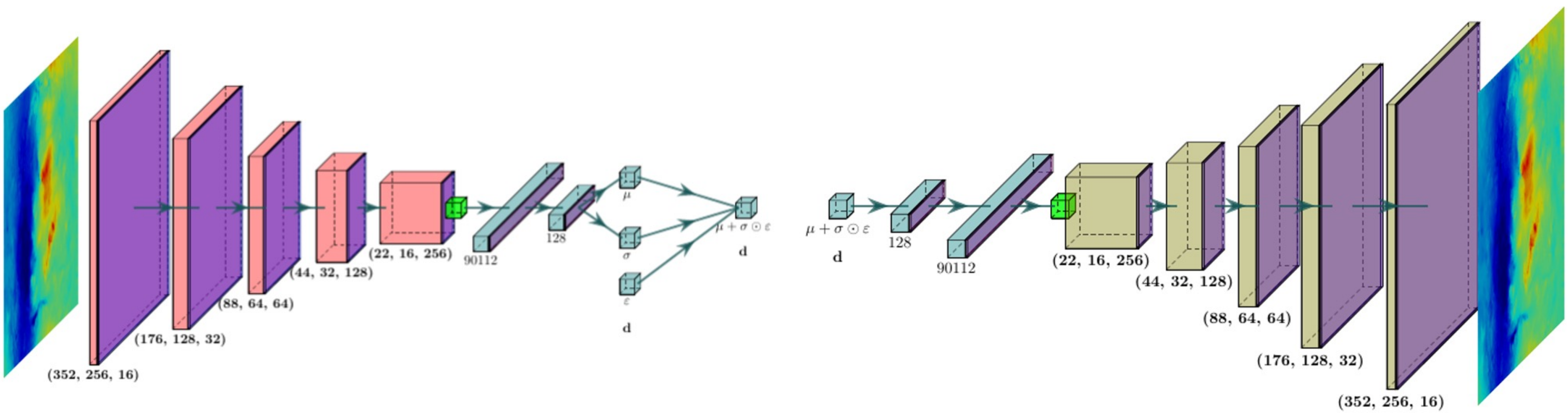

B. Eiximeno, A. Miró, I. Rodríguez, and O. Lehmkuhl, "*Mathematics*, vol. 12, no. 7, pp. 1–23, 2024.

Data analysis: Deep Learning Surrogate Models

Windsor body at $Re_L = U_\infty L/\nu = 2.9 \times 10^6$

WMLES results

δ=7.5º

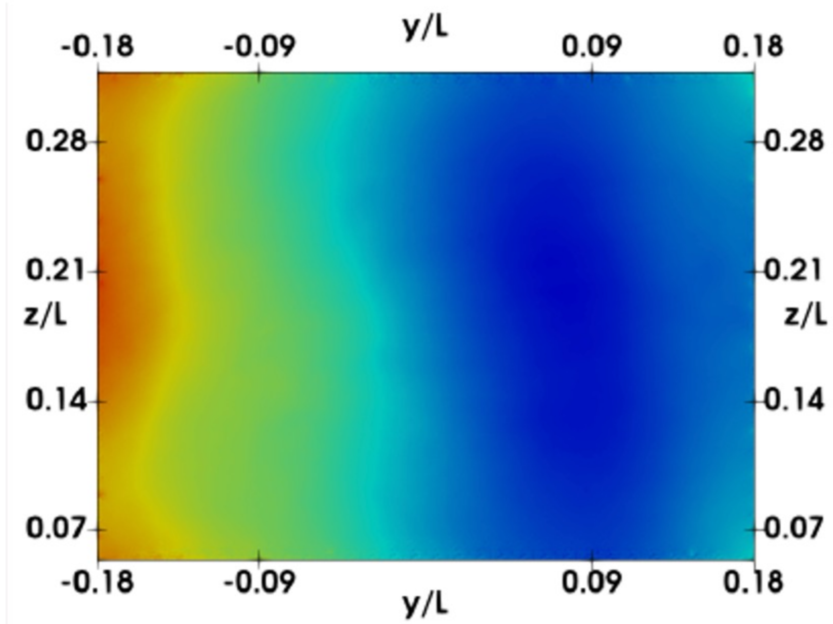

The projection of the mean pressure coefficient value through the encoder, leads to a linear evolution of the latent variables with the yaw angles

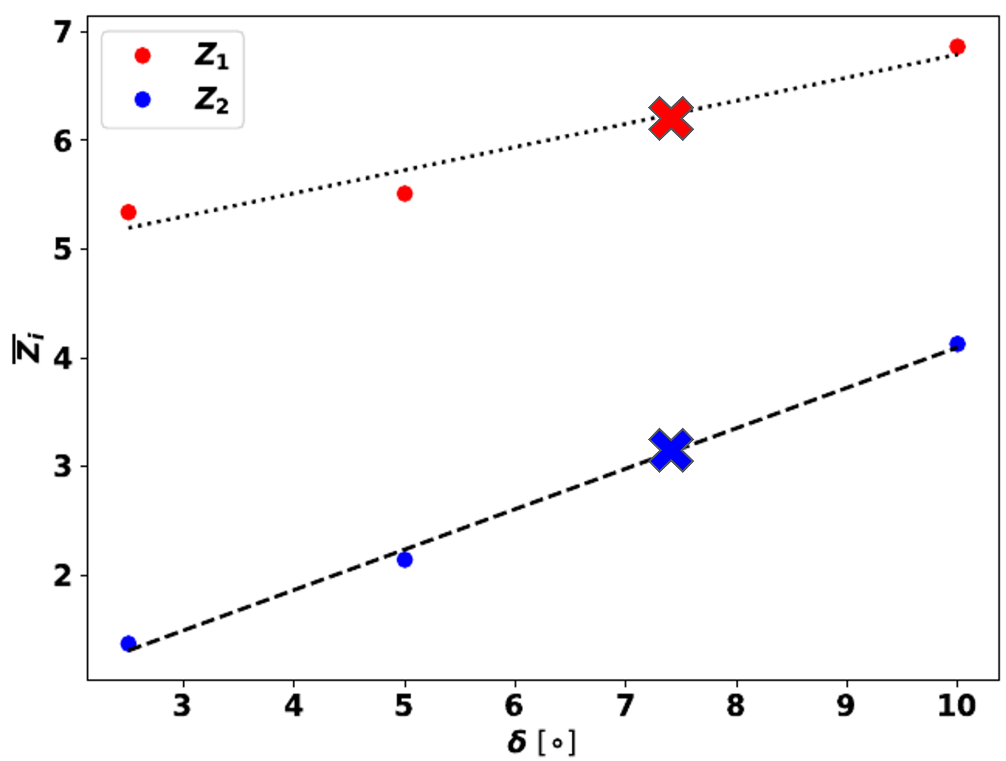

Projection of the interpolated latent variables through the decoder

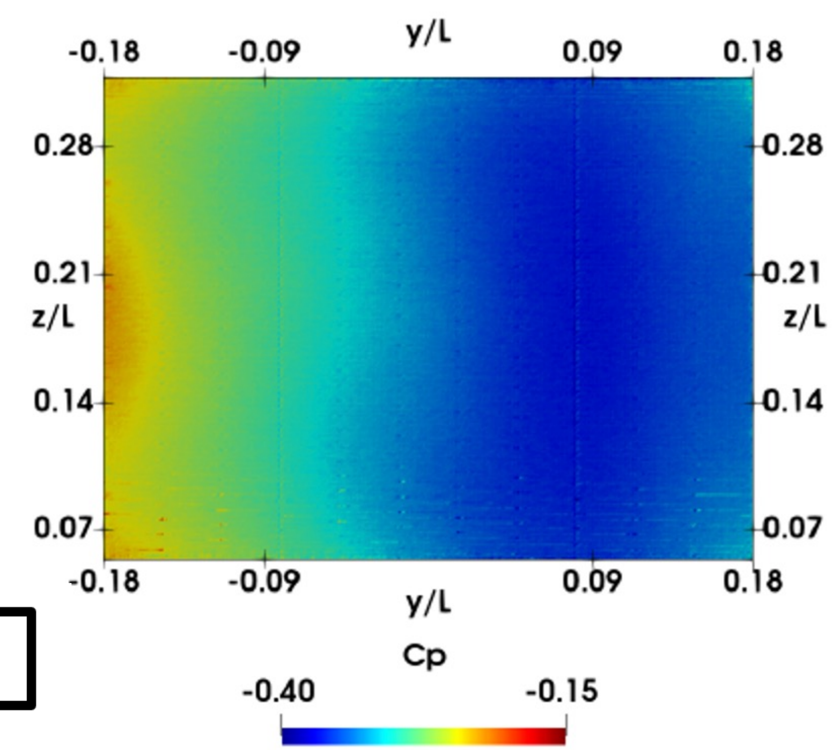

So we can get the value of the latent variables in this range with a linear regression

Mean error between both is of 3%

B. Eiximeno, A. Miró, I. Rodríguez, and O. Lehmkuhl, "*Mathe*

Data analysis: Deep Learning Surrogate Models

Windsor body at $Re_L = U_\infty L/\nu = 2.9 \times 10^6$

$\delta = 10^\circ$

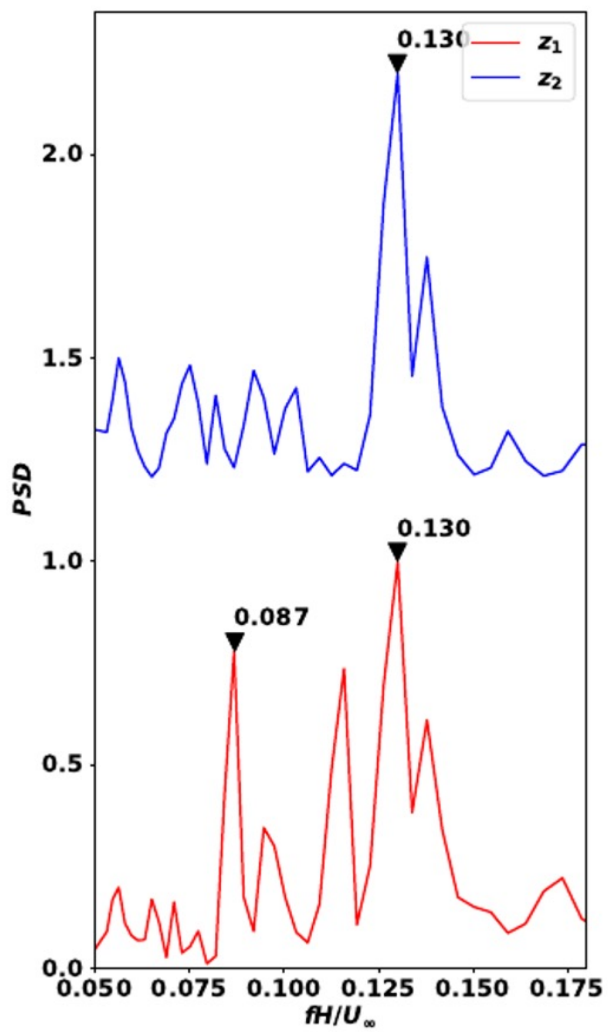

Spectra of the latent space

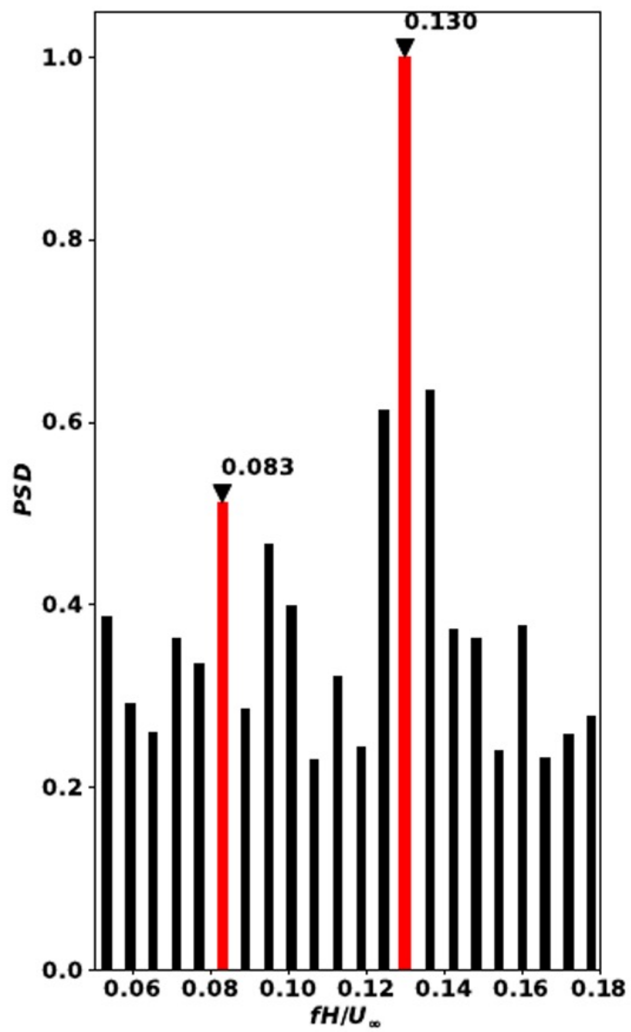

Frequency of DMD modes

The temporal evolution of the latent vectors was assessed. 660 snapshots of the back pressure at each yaw angle δ = [2.5º, 5º and 10º]

- The snapshots of each angle have been projected through the encoder while keeping the time correlation
- The temporal evolution of the latent space has the same dominant frequencies as the most relevant modes of the dynamic mode decomposition

flow dynamics is preserved in the latent space

B. Eiximeno, A. Miró, I. Rodríguez, and O. Lehmkuhl, “*Mathematics*, vol. 12, no. 7, pp. 1–23, 2024.

Data analysis

POD/DMD to detect the noise sources in the near field + FWH

Re=10000 M=0.8 (LES)

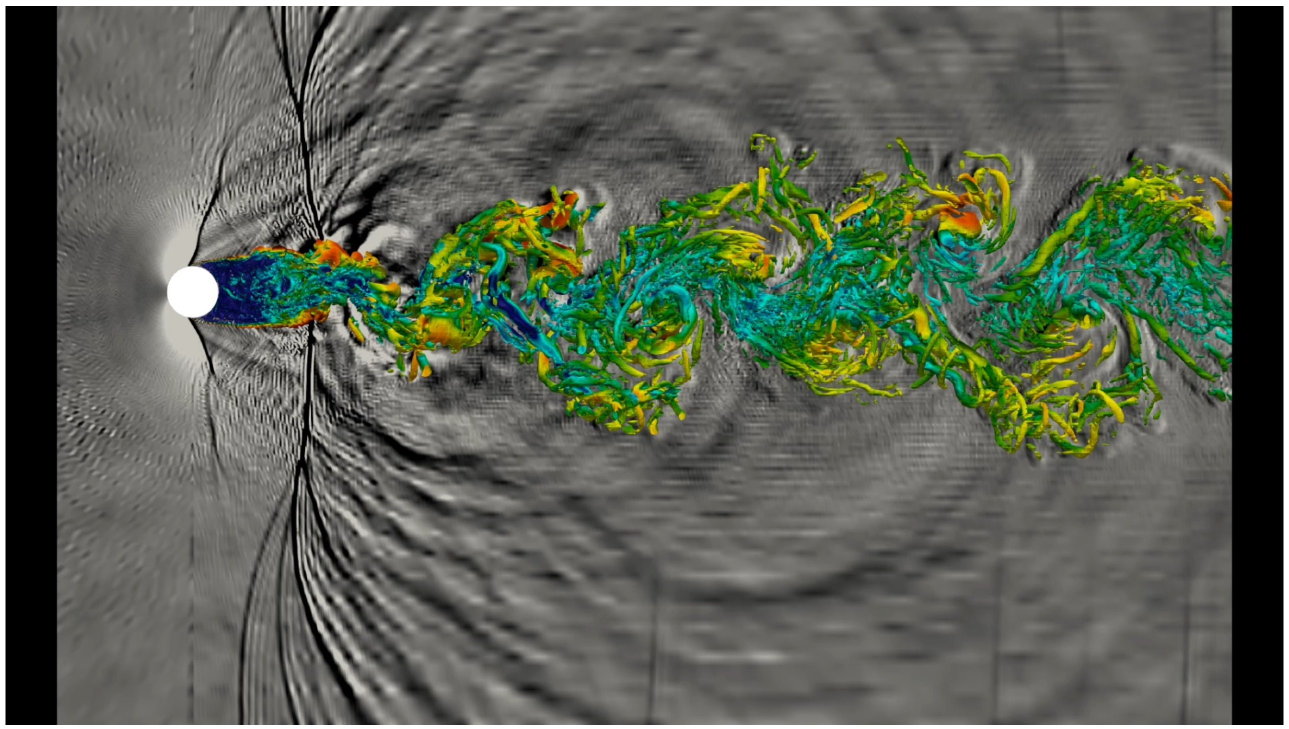

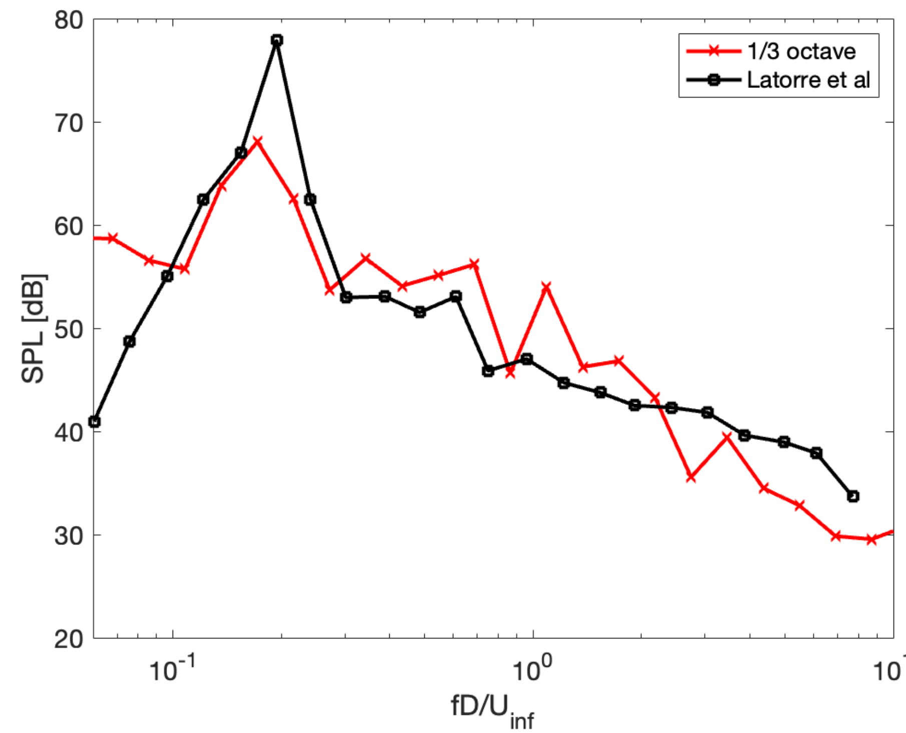

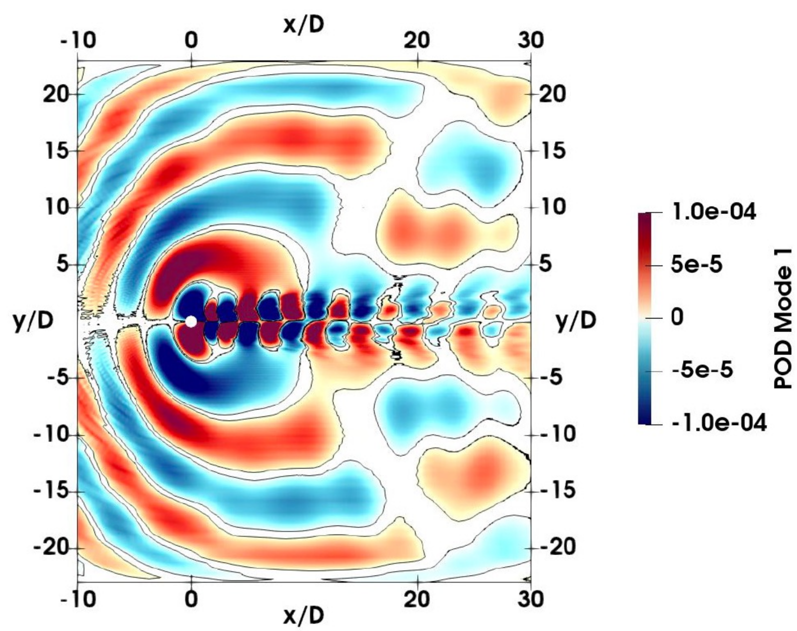

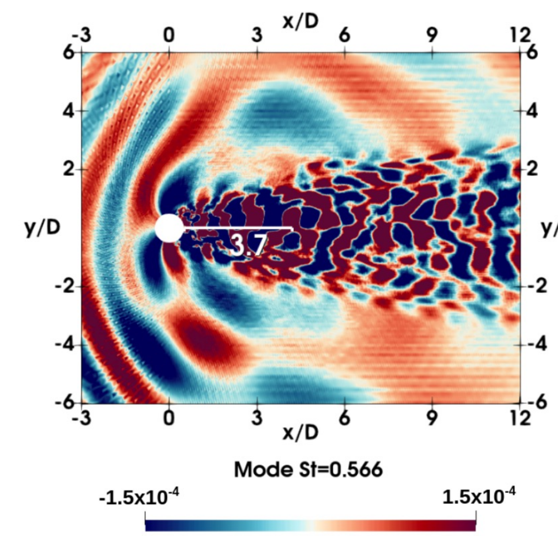

(b)

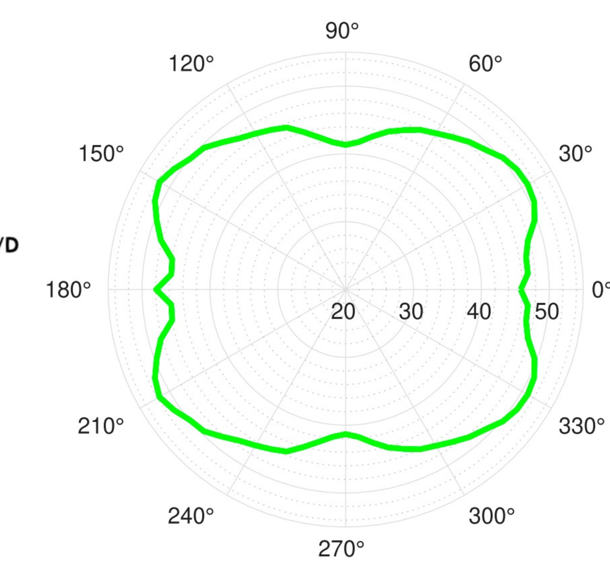

(c)

Summary

- High-fidelity simulations of complex flows can be performed using low-dissipation methods
- At high Reynolds numbers WMLES is affordable with rather good accuracy
- AFC for external aerodynamics show promising results, DRL-based AFC can be a means for discovering new strategies and deal with the large number of parameters to optimise
- Data analysis via ROMS can be used for identification of main coherent structures, noise sources and possible as subrogate models for drag prediction or finding best flow control strategies

THANK YOU FOR YOUR ATTENTION

EuroHPC Joint Undertaking

RED ESPAÑOLA DE SUPERCOMPUTACIÓN

GOBIERNO DE ESPAÑA

MINISTERIO DE CIENCIA E INNOVACIÓN

VEGA HPC

Barcelona Supercomputing Center
Centro Nacional de Supercomputación

AGAUR
Agència de Gestió d'Ajuts Universitaris i de Recerca

UNIVERSITAT POLITÈCNICA DE CATALUNYA BARCELONATECH

TUAREG
Turbulence and Aerodynamics Research Group